water

MDPI

Article

A New Metric for Assessing Resilience of Water Distribution Networks

Ahmed Assad [1,*], Osama Moselhi [1] and Tarek Zayed [2]

[1] Department of Building, Civil and Environmental Engineering, Concordia University, Montréal, QC H3G 1M8, Canada
[2] Department of Building and Real Estate (BRE), The Hong Kong Polytechnic University, Kowloon ZN716, Hong Kong, China
* Correspondence: ahmed.assad@mail.concordia.ca

Received: 22 June 2019; Accepted: 14 August 2019; Published: 16 August 2019

Abstract: Water distribution networks (WDNs) face various types of hazards during their extended life. Ensuring proper functioning of WDNs has always been a major concern for utility managers because of their impact on public health and safety. Resilience is an emerging concept that aims at maintaining functionality of the WDNs. Most of the previously developed resilience frameworks employed simulation methods to assess resilience of the WDNs, focusing only on the specific aspects of resilience. There is a need to develop a holistic approach to evaluate the resilience of WDNs considering various dimensions of resilience. This paper presents a new multi-attribute resilience metric based on the robustness and redundancy of the WDNs, which can be used to achieve the purpose. The developed metric is used to evaluate the resilience of a WDN in the city of London, Ontario. An optimization framework for enhancing the current resilience level is also presented. Resilience of the network is found to increase around 20% with a $500,000 investment. A hazard scenario is then analyzed to illustrate the practicality of using this metric in selecting effective restoration strategies. The proposed metric can be utilized by water agencies to evaluate and enhance the resilience of WDNs, as well as to optimize the recovery process after disruptive events.

Keywords: resilience; water distribution networks; critical infrastructure; multi-attribute metric

1. Introduction

Water distribution networks (WDNs) are critical infrastructure systems that are responsible for securing adequate quantities of safe, high-quality water to the public [1]. Maintaining a proper functioning of the water systems has always been a primary concern for cities and municipalities because of their direct impact on the health and safety of the people [2]. Following any hazard, water infrastructures play a dominant role in firefighting and other rescue efforts. Thus, attaining functionality of such critical systems is a more appealing demand after any hazard event [1]. During their extended service life, WDNs face a broad spectrum of hazards that disturb their functionality and potentially threaten human survival. These hazards that are becoming more frequent and of more damaging consequences are either natural disasters or human-made ones. Earthquakes, floods, hurricanes, extreme temperatures, and climate change are examples of natural hazards that affect the WDNs. Human-made risks may include terrorist attacks, cyber-attacks, overloading, and vandalism [3]. Aging and deterioration of WDNs increase their vulnerability and the likelihood of function interruption during and after the disruptive events. Pipe breaks, loss of pressure, leaks, and contaminants entering the network are all instances of such consequences [3]. Traditionally, the focus was placed on physical protection of water systems by avoiding or mitigating the likelihood of disruptive events and their adverse impacts [4]. However, because of the high uncertainty nature of hazards and complex

interdependency of infrastructure systems, it is not possible to protect water networks from all hazards using classical strategies. Therefore, infrastructure resilience is emerging as an essential consideration in the planning and management of WDNs. In this context, water networks will be strong enough to withstand any disruption with a minimum impact on its performance and to recover quickly in case of service loss [4]. Resilience capabilities in infrastructure systems are usually described by three main aspects, namely: absorptive, adaptive, and restorative capacities [5]. Absorptive capacity measures the ability of a system to withstand the impact of a hazard event with minimum disruption in the services it provides. Adaptive capacity measures the system's capability to adjust itself under a new disrupted state and to continue delivering its service. Restorative capacity is a measure of the system's ability to recover efficiently. The American Society of Civil Engineers defines resilience of infrastructure systems as the ability to mitigate all-hazard risks and rapidly recover critical services with minimum harm to the public safety, health, economy, and national security [6]. This definition, among others reported in the literature, interprets resilience of infrastructure systems as a process that inherits the four distinct phases. The process always starts with some preparedness measures to mitigate the impacts of anticipated hazards. After the occurrence of a hazard event, a response process starts, and recovery actions are taken to restore the service. Subsequently, policies are revised to be better prepared for the next hazard events.

The literature includes various models and frameworks that evaluate the resilience of water systems and WDNs. Approaches in this area can be broadly classified into two main categories: qualitative approaches and quantitative approaches [2]. Qualitative approaches can be either in the form of conceptual frameworks or as semi-quantitative indices [7]. Fisher et al. [8] developed an index to measure the resilience of critical infrastructures, including water systems. The model involved extensive data collection of about 1500 variables categorized under robustness, recovery, and resourcefulness. The variables were then weighted and summed to generate a single global resilience index that allows the comparison between different infrastructure systems [8]. Fiksel et al. [9] developed another example of conceptual frameworks to evaluate the resilience of water systems by assessing several factors such as vulnerability, recoverability, resource productivity, cohesion, adaption, and diversity. Such approaches are usually subjective, and the results cannot be generalized on a large scale of water systems. Quantitative approaches for measuring resilience may also be classified as either probabilistic or deterministic depending on whether the stochastic nature of the system functions is considered. Each approach can be further clustered as a dynamic approach or a static one. The former considers the time-dependent functions of a system, while unlike the latter [2]. Todini [10] introduced a resilience metric as a measurement of the excess power in a system and demonstrated its applicability in the design of WDNs. Jayaram and Srinivasan [11] extended Todini's metric to account for multiple sources in network resilience quantification. In their research study, the authors obtained a trade-off between life-cycle cost and modified resilience index using multi-objective optimization. The life cycle cost comprised of installation cost, replacement cost, cleaning and lining cost, breakage cost, and salvage value. The authors simulated a sample network over an extended period while increasing the roughness of water pipes to capture the hydraulic deterioration of the network. The authors reported considerable cost savings by considering the design and rehabilitation together instead of exclusively focusing on overdesigning the network. Suribabu [12] utilized the previous two metrics to optimize the design of WDNs. In his work, he considered minimizing the cost of network resilience enhancement subject to specific pipe diameters and pressure head constraints. The optimization model suggested configuring the network such that the pipe sizes are decreasing along the shortest path. In a different research study to optimize the design of WDN, Choi and Kim [13] formulated a multi-objective model that considers mechanical redundancy under multiple pipe failures of different states. The study derived a relationship between pipe failure states and mechanical redundancy. Also, the authors analyzed, through simulation, the demand levels of abnormal situations based on extreme demands. In that study, system hydraulic ability was used as an indication of the system's redundancy; however, other redundancy measures of topological

characteristics can be used. Another extension of the resilience index proposed by Todini can be found in a study presented by Creaco et al. [14]. In his study, Creaco et al. [14] extended the original resilience index by using pressure-driven modeling and accounting for the energy dissipated by leaks through the water pipes. The authors studied time variation of resilience resulting from changing pipe leakage and roughness coefficients while investigating the cost of the network. The reported cost and delivered power of the configuration obtained after these modifications outperformed the corresponding values obtained by the original index suggested by Toodini [10].

Bruneau et al. [15] developed one of the most widely used metrics for resilience assessment. In their work, the authors calculated the resilience loss, *RL*, as a deterministic dynamic metric that captures the degradation of a system following a hazard event, Equation (1).

$$RL = \int_{t_0}^{t_1} [100 - Q(t)]dt \tag{1}$$

where *RL* is the resilience loss, $Q(t)$ is a quality function that measures the system performance as a percentage, t_0 is the time at which the disruption occurs, and t_1 is the time at which the resilience is calculated. $Q(t)$ can be any performance indicator of the system. In this method, the initial performance of the system is assumed to be 100, and the shaded area represents the resilience loss, as shown in Figure 1 [15–17]. An extension of this method is found in the research effort done by Henry and Ramirez-Marquez [18]. The authors defined three distinct states, namely: original stable (S_0), disrupted (S_d), and stable recovered (S_f) that depict the states of any system before, during, and after the occurrence of a hazard, respectively. Equation (2) is used to calculate the resilience as a ratio between the recovery level at any instant to the initial loss in the performance function [18–21].

$$\mathcal{R}_F(t_r|e_j) = \frac{[F(t_r|e_j) - F(t_d|e_j)]}{[F(t_0) - F(t_d|e_j)]} \tag{2}$$

where $\mathcal{R}_F(t_r|e_j)$ is the proportion of delivery function that has been recovered from the disrupted state under event e_j, $F(t_r|e_j)$ is the figure-of-merit of the system at the recovered state t_r, $F(t_d|e_j)$ is the figure-of-merit of the system at the disrupted state t_d under the event e_j. Dessavre et al. [21] formulated a five-states resilience framework for assessing the resilience of urban infrastructure systems before, during, and after the disruption events. Figure 2 illustrates their model, starting from a steady reliability state when a system functions normally before the occurrence of a disruptive event. At that instant, the system undergoes a transition state beginning with a gradual reduction in its performance, followed by an idle period for damage estimation and restoration planning. This transition finally ends by a course of recovery actions to restore service provision. The final recovered steady state may be either same, less, or even more than the initial state before the disruption occurrence [21].

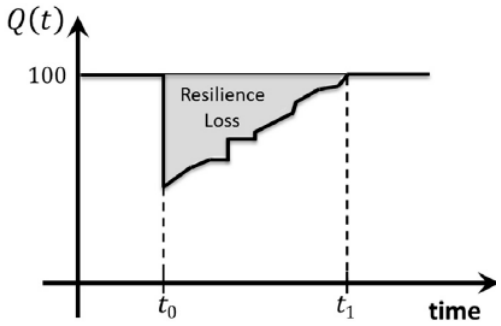

Figure 1. Resilience loss measurement [15].

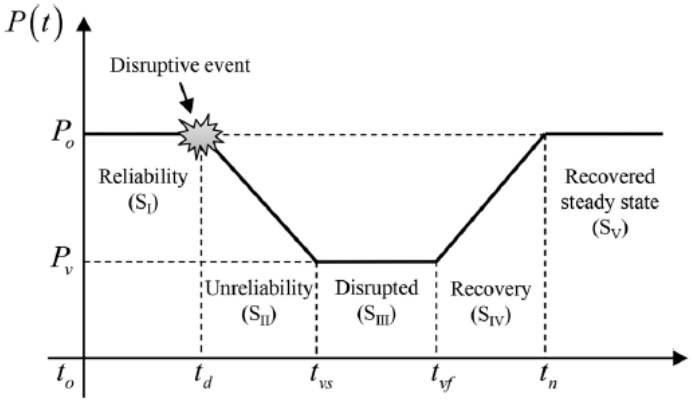

Figure 2. Engineering resilience curve [21].

Ouyang et al. [22] extended previous approaches to present a stochastic time-dependent metric for measuring the annual resilience against multi-hazard events. This metric, given in Equation (3), measures resilience as the mean ration between the actual performance curve, $P(t)$, and the target performance curve, $TP(t)$, over a time period (T) which equals one year in the original model.

$$AR = E\left[\frac{\int_0^T P(t)dt}{\int_0^T TP(t)dt}\right] \quad (3)$$

where AR is the annual resilience and E is the mean operator. Zhao et al. [23] employed this time-based resilience measure to compare the technical and organizational effects of two post-disaster rebuilding strategies: pipeline ductile retrofitting and network meshed expansion. They concluded that retrofitting is a preferred strategy to enhance seismic resilience of WDNs under limited recovery budget and resources, whereas meshed expansion can increase the performance of WDNs in the case of sufficient fund availability. Several previous studies followed an approach of depicting resilience as the antonym of system vulnerability [24,25]. For example, Baroud et al. [24] developed a model to assess the resilience based on vulnerability and recoverability of waterway networks. The authors employed two stochastic measures to rank the links in a network based on their importance. A multicriteria comparison technique was utilized to produce the order of the ranked components. Other authors compared the resilience index and the entropy index in rehabilitation planning of WDNs. For example, Cimorelli et al. [26] suggested a rehabilitation methodology to increase two surrogate reliability measures subject to a limited budget. They compared the performance of the resilience index suggested by Creaco et al. [14] and entropy index based on two case studies. The authors found that the considered resilience index is more accurate in reliability estimations. It was also recommended to consider demand satisfaction when using the entropy index in constrained budget rehabilitation of WDNs. In some studies, indicators from graph theory were employed, such as connectivity, link density, meshed-ness, spectral gap, and central-point dominance to provide quick and practical resilience indicators [27–29]. Some authors focused their studies on the loss estimation and restoration efforts in the context of seismic resilience [30,31]. Farahmandfar et al. [31] compared the performance of topology-based and flow-based metrics in optimizing the selection of rehabilitation strategies of large WDNs which are prone to seismic hazards. The decision variables included a combination of pipeline replacements and new pipeline installations. The objective was to achieve the maximum enhancement of resilience given a capital budget constraint. The results indicate that the flow-based metric is relativity more accurate; however, it is suffering from significant computational time.

Consulting the literature about resilience assessment of WDNs reveals several remarks. Generally, more efforts focused on incorporating resilience in the design phase of WDNs compared to incorporating resilience during the operation and maintenance of WDNs. Most of these models depend mainly on running complex hydraulic simulations. The main issue with hydraulic simulation-based methods is

that they require complicated calculations and parameters calibration, which significantly increase the computational cost, especially as the size and complexity of the network increase [32]. Many researchers have tackled resilience from a disaster management perspective, "a snapshot in time" disregarding some important asset management concepts such as deterioration and aging of water networks [33]. Research efforts that investigated such concepts usually tend to assume the expected level of deterioration. For example, both Jayaram and Srinivasan [11] and Creaco et al. [14] investigated the effects of deterioration through hydraulic simulation by increasing the roughness of water pipes. However, the rates of roughness growth were assumed in both studies. There is still a need to adopt more accurate methods in estimating the deterioration of WDNs. This will facilitate investigating a long-term variation of resilience during the operation phase, which will help guide the investments in WDNs and preparedness plans.

On the other hand, approaches based on graph theory rarely consider other non-topological characteristics of WDNs such as pipe lengths, diameters, aging effects, and previous failure history. Including such factors yields better estimates of resilience levels of the WDNs, which will help in deriving optimum enhancement and restoration plans. Additionally, most of the previous research studies that investigated the probability of failure were limited to analyzing one specific source of hazard, such as earthquakes. There is a need to shift the emphasis to analyze the impact of risks on the network, which will facilitate addressing several hazards that result in the same impacts in one single analysis. Furthermore, few efforts have considered various dimensions of resilience in a single metric that can be readily used in real-world applications. For example, some components might be of a higher economic and social criticality (e.g., pipe segments delivering water to hospitals) and require a more rapid recovery than other components.

The objective of this paper is to present a newly developed metric for assessing resilience of WDNs that overcomes the previous limitations, and to demonstrate its applicability in selecting efficient enhancement and recovery strategies. The rest of this paper is organized as follows: In Section 2, the multi-attribute resilience metric is introduced where the underlying concepts and mathematical formulation are presented in detail. In Section 3, the developed metric is used to evaluate the resilience of an actual WDN in the City of London, Ontario. An optimization framework is then presented to select the optimal resilience enhancement plan. This section also includes a hypothetical example to illustrate the practicality of using the proposed resilience metric in selecting the best restoration strategy. The computed resilience levels are then compared to values obtained by previously developed metrics. Conclusions are drawn in Section 4 along with the research limitations and recommendations for future studies.

2. Research Methodology

In this work, a multi-attribute metric for assessing resilience of WDNs is presented. This work is based on a comprehensive framework presented by Bruneau et al. [15] for analyzing the resilience of urban communities and infrastructure systems. Generally, resilience of infrastructure systems can be conceptualized as having four main qualities, namely: robustness, redundancy, rapidity, and resourcefulness [15,30,34]. The first two properties are integrated in this work to offer a new practical resilience metric. The aim is to provide a metric that can be readily used by utility managers to estimate resilience of WDNs. Figure 3 illustrates the overall methodology of developing this metric. The method starts by collecting some data from different sources, including interviews with experts, literature reviews, and database of the City of London, Ontario. In this model, robustness is estimated as a function of the reliability and criticality of water pipes. Redundancy is calculated by utilizing concepts of graph theory. The detailed assumptions, definitions, and analytical quantifications of each attribute of this resilience metric are presented in the following subsections. The metric is then used to estimate the current resilience level of an actual WDN in the City of London, Ontario. Subsequently, an optimization model is formulated to investigate the different resilience improvement actions and to select the optimal resilience enhancement plan. The practicality of using the proposed metric

in resilience restoration applications is then demonstrated by assuming a specific disruption event and investigating various restoration strategies. It should be noted that the metric developed in this work will serve as a first step toward building a comprehensive resilience-based asset management methodology for WDNs. Following steps develop optimization models that integrate the concepts of rapidity and resourcefulness. The aim is to enhance the current resilience level and to assist in selecting the optimal restoration strategy that minimizes the time and cost of service interruption following a hazard event.

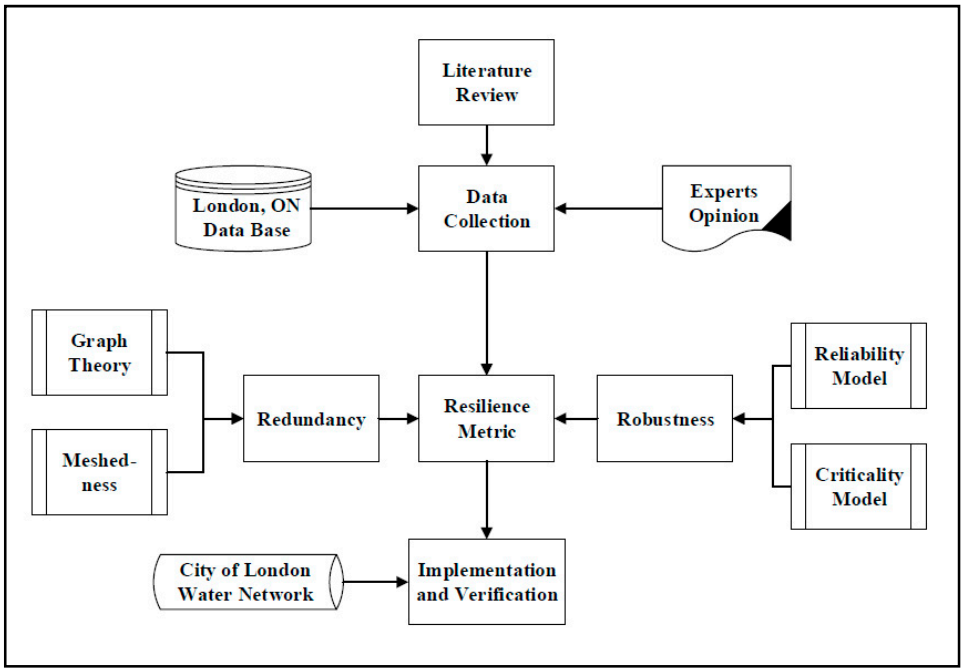

Figure 3. Resilience metric development methodology.

2.1. Robustness

Robustness of WDN is its ability to withstand disaster forces without significant degradation [35]. Robustness can be sought as the resistance to an unusual external shock often measured by the residual functionality level after the occurrence of the event [35]. In this work, mechanical reliability is chosen as the base for quantifying the robustness of a WDN as it is a direct measure of its structural performance. Mechanical reliability is the "probability that an item can perform its intended function for a specified interval under stated conditions" [36]. In this work, reliability will be used to refer to the mechanical reliability. Structural performance of WDNs is a measure of the structural condition of its components. A pipe burst or a pump malfunctioning may then compromise the structural performance of WDNs and decrease its reliability [36,37]. Moreover, a deteriorated pipe segment with long failure history is more fragile/vulnerable to even light disruptions. Robustness is thus calculated as the sum of the reliabilities of all the connected pipe segments. Criticalities of pipe segments are then added as weights to prioritize critical segments. For a network that consists of several pipe segments, the most critical segments are the most important ones in determining its performance. Finally, the weighted formulation is normalized by the sum of criticalities of all pipe segments. By adding criticalities, the developed resilience metric is extended to account for the social and economic dimensions of resilience beside the technical one that is captured in the reliability of pipe segments. Detailed descriptions of calculating the criticality and reliability of water pipe segments are provided below.

2.1.1. Criticality

Asset Criticality is a measure of the consequences associated with the failure of an asset to perform its intended function [38,39]. The first step in estimating criticality of water pipe segments is to identify some factors, known as criticality factors. A criticality factor is a characteristic that impacts the consequence of a pipe segment failure. For example, the size of a pipe segment is considered a criticality factor because it affects the economic consequence associated with this segment failure. Based on the type of potential consequences, criticality factors can be classified into main categories such as economic, environmental, and social factors. A factor can be assigned to one or more categories if it impacts the type of consequences represented by that category. For example, the size of a pipe can be categorized as both economic factor and social factor. Moreover, social consequences may contribute in increasing the economic effects. Thus, there is a kind of interdependency between these factors. Previously, several researchers tried to estimate criticality of water segments [40–42]. However, these efforts are still subjected to uncertainty, bias, and lack of knowledge inherited by the decision-makers [40]. Thus, there is a need to estimate criticality of water pipe segments while considering the uncertainties and interdependencies between the criticality factors. Data needed for developing this model include factors affecting criticality of water pipe segments, relative importance of these factors, and scores for measuring each one of them. Figure 4 illustrates a flow diagram that summarizes the criticality estimation steps. Based on the type of potential losses, three main categories of criticality factors are included in this study, as shown in Figure 5. Economic factors measure the monetary losses realized after a water pipe failure. These losses can be quantified as increased repair costs or loss of revenues. This category includes pipeline size, material, installation depth, and accessibility. As the size of a water pipe increases, the monetary losses associated with its failure increase due to the higher repair cost. The same can be said about the depth at which the water pipe is buried. According to Salman [40], the repair cost increases dramatically when the failed water pipe is buried at a depth exceeding four meters. Moreover, the pipe material will dictate the repair type and methodology. Hence, it directly affects the cost of the failure and repair actions. Concrete pipes usually have more repair cost than other material types [40]. Additionally, the failure of a pipe segment that is not easily accessible leads to more significant losses.

Environmental factors are those that measure the environmental impacts resulting from a water pipe failure. These impacts can be in the form of health impacts, contamination, pollution, and others. In this category soil type, proximity to water streams, and pipeline size are the sub-factors included. It is well-known that pipe segments closer to water streams such as rivers and lakes are more critical because of the possible contamination that might result from their failure. Additionally, environmental impacts increase gradually as the size of the failed water pipe increases because of the higher amount of discharged water. Each soil type has its permeability and density characteristics that control the amount and spread of the consequences resulted from a water pipe failure. Failures in sandy soil are considered more critical because of the possibility of runoffs and adversely affecting adjacent facilities. Social factors include sub-factors that influence the social disruptions exhibited because of the failure of the water pipe. Population density, traffic disruption, existing alternative route, and type of the serviced area are the sub-factors considered in this cluster. Social impacts are increased as the population density increases owing to the larger number of affected users as a result of a pipe failure. A pipe segment that is under, or close, to a highway is more critical than those buried in small local roads because of a higher volume of traffic that is being disrupted. Also, the availability of an alternative path to deliver water to the demand node reduces the criticality of this pipeline. Furthermore, water pipes that deliver water to sensitive facilities such as hospitals and power plants are more critical than others. Failure in such segments has more negative impacts on the society and may take longer time to recover because of the propagated effects resulting from insufficient water supply to those facilities.

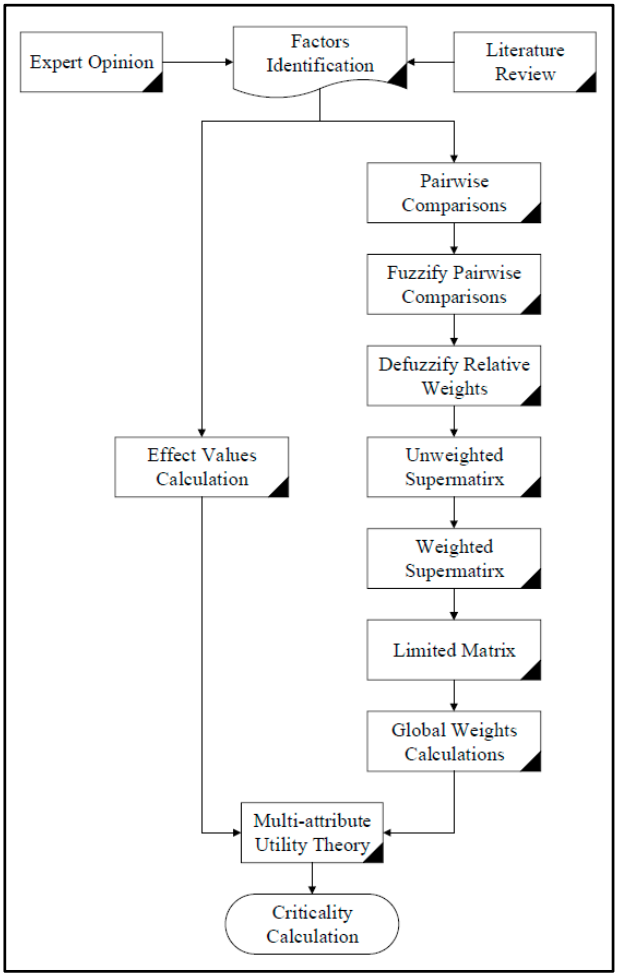

Figure 4. Flow diagram of criticality assessment process.

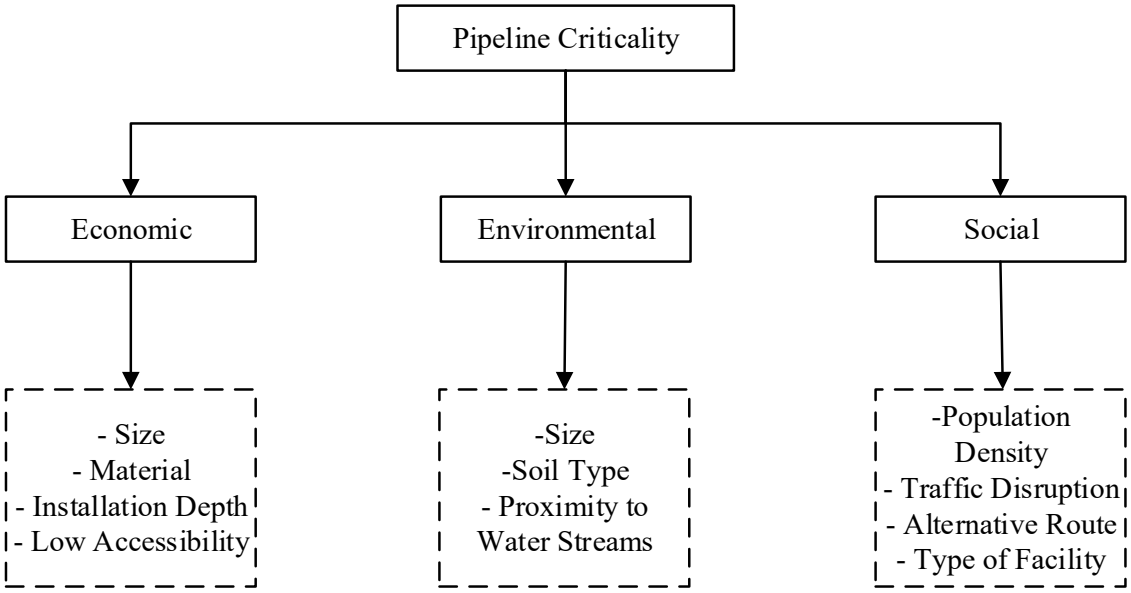

Figure 5. Criticality factors and sub-factors.

Criticality estimation constitutes using a diverse set of factors, not all of which are measured on comparable scales. These factors are measured on a binary scale, continuous range, or discrete

categorical interval. It is thus necessary to define a unified scale, effect value, that allows for a meaningful combination of the different factors in a multi-attribute utility model. After identifying criticality factors, experts' opinions were sought to derive the relative weight of importance of each sub-factor and to determine the effect values on pipe segment criticality on a scale from 0–10. Table 1 shows the effect values of economic criticality subfactors. In Table 1, accessibility is measured on a binary scale as either high or low. Thus, only two effect values are considered 1 and 10 representing the least and most critical conditions respectively, without considering any intermediate conditions. Effect values that represent these intermediate conditions are marked as NA. The same approach was followed for the installation depth criticality factor. Similar values were collected for environmental and social factors.

Table 1. Effect values of economic criticality factors.

Affect Value	Pipeline Size (mm)	Pipe Material	Installation Depth (m)	Accessibility
1	Less or equal 150	PVC, Polyethylene	Less 4.0	High
3	150 to 350	NA	NA	NA
5	350 to 700	Steel, Iron	NA	NA
7	NA	Copper	NA	NA
10	Greater or equal 700	Concrete	Greater or equal 4.0	Low

Fuzzy analytical network process (FANP) is then employed to obtain the global weights of the influential factors. FANP belongs to the family of multi-criteria decision-making (MCDM) problems. MCDM refers to achieving the best alternative among all feasible options based on multiple decision criteria [43]. FANP is a technique that combines ANP, fuzzy theory, and fuzzy analytical hierarchal process, fuzzy AHP. This technique accounts for inner and outer interdependencies, uncertainty, and imprecision in decision-making. Thus, utilizing FANP overcomes the limitations on previous efforts that attempted to estimate criticality of water segments. The process starts by identifying the system objective and sub-criteria, which has been done in the last step. The aim is to calculate criticality index of water segments, and the criteria are the main factors and subfactors considered. Subsequently, a comparison between criteria is performed on a pairwise basis. This is done by asking, "How much importance does a criterion have, compared to another criterion concerning our interests or preferences?" [44]. Experts were asked to compare the factors via linguistic terms as shown in Table 2. The fuzzy component is implemented by applying a fuzzification scale on the gathered responses. Cheng's fuzzy scale is exploited in this study for pairwise comparisons and fuzzified weights computations [45–47]. This application yields formulation of three matrices, namely: lower, most probably, and upper matrices which represent the three vertices of a triangle fuzzy number. Triangle fuzzy membership function is utilized in this application as it is the most commonly utilized one in literature. Moreover, this function fits for the objective of this application, where three points are sufficient to describe the inherited uncertainty. For example, if an expert evaluated factor A to be weekly more important than factor B, the mean value of the fuzzy membership function associated with this evaluation response is 3/2. Furthermore, the corresponding lower and upper values associated with this response will be 1 and 2 respectively. This step will be repeated to compare between all the sub-factors in each category and between the three main considered categories. The output of this step is a set of lower, upper, and most probable matrices for each evaluated comparison. The application of this fuzzifying scale is to account for the vagueness and uncertainty in the collected responses. These matrices are then used as inputs for a Matlab code to obtain the factors' relative weights. Subsequently, the obtained defuzzified relative weights are used to construct the unweighted supermatrix. The weighted supermatrix is next attained by normalizing each column in the unweighted supermatrix to the summation of its cells. This step is similar to the concept of Markov chains for ensuring the sum of probabilities of all states is equal to one. The weighted supermatrix is raised to considerable powers till convergence, the resulting matrix is the same as the raised ones, to get the limited matrix, as shown in Equation (4). The first column in the limited matrix is the global

priority vector or weights [44]. Summing up the weights obtained from the limited matrix yields to an exact unity.

$$\overline{W}^{\infty} = \lim_{k \to \infty} \overline{W}^{k} \tag{4}$$

Table 2. Cheng's fuzzy linguistic scale for importance and the corresponding triangular fuzzy numbers [45].

Linguistic Scale for Importance	Triangular Fuzzy Scale	Triangular Reciprocal Scale
Equally important (EI)	(1/2,1,3/2)	(2/3,1,2)
Weakly more important (WMI)	(1,3/2,2)	(1/2,2/3,1)
Strongly more important (SMI)	(3/2,2,5/2)	(2/5,1/2,2/3)
Very strongly more important (VSMI)	(2,5/2,3)	(1/3,2/5,1/2)
Absolutely more important (AMI)	(5/2,3,7/2)	(2/7,1/3,2/5)

Multi-attribute utility theory (MAUT) is employed to find the criticality index of each pipe segment using Equation (5). A Matlab code that is integrated within an Excel environment was written to automate the criticality computations.

$$C_i = \sum\nolimits_{j=1}^{r} W_j \times AV_j \tag{5}$$

where C_i is the criticality index for pipeline i, W_j is the global weight of criticality sub-factor j, AV_j is the effect value of sub-factor j, and r is the number of criticality sub-factors. Criticality index reflects the significance of water pipe failure on a scale from 0–1, where 0 represents the least critical, and 1 represents the most critical pipe segments.

2.1.2. Reliability

Reliability is defined as the probability that an infrastructure system, or any of its components, will perform its intended function without failure for a specified period [37]. A failure in water pipe segment could be either a hydraulic failure, a structural/mechanical failure, or a failure related to water quality issues [48,49]. The only type of failure considered in this paper is a structural failure in the form of pipe breaks. Other types of pipe failures can be included as future extensions to this study. The general form to calculate the reliability of an asset is given by Equations (6) [36]:

$$R(T) = P(t > T) = 1 - \int_{T}^{\infty} f(x)dx \tag{6}$$

where t is the time to failure, T is the period of failure-free, $f(x)$ is the failure probability density function. The steps of reliability and deterioration estimation are illustrated in Figure 6. Data needed for calibration of this model include characteristics, locations, and failure history of water mains. These data were gathered from the City of London, Ontario. Once data are collected, preprocessing steps are performed as follows:

1. Data cleansing is first done to eliminate any miscoded or irrational data like those whose installation date, or failure date is sometime in the future.
2. Pipes that have significant time to the first failure are excluded from modeling. This step is essential to avoid the bias resulting from intervention and major rehabilitation works that were implemented but not reported in the database.
3. The number of breaks in each pipe segment is counted and linked to that specific pipe. The gathered data included several GIS layers that were not spatially linked to each other. Hence, a Matlab code is written to count the number the breaks and match them to the appropriate pipe segment utilizing features of Arc-GIS.

4. The inter-failure time, the time between successive failures, is calculated to get times to the *n*th failure. These times will be used later to calibrate the model and determine the best fit.

The concept of censored data is utilized in this research. The most generic form of censoring is right-censored data. In this case, the failure event starting the inter-failure time series has occurred, but at the time of the last update of the data, the failure ending this series has not occurred yet. The only thing known for sure is that the failure will happen sometime in the future. The main advantage of employing data censoring is the ability to include the effect of no-failures in addition to the effect of failures. Water pipes are then clustered into homogeneous cohorts based on the material type and size. Five main groups resulted from this clustering, namely: mains that are made of cast iron, CI and of a diameter less than or equal to 150 mm; mains that are made of CI and of diameter more than 150 mm; mains that are made of ductile iron, DI and of diameter less than or equal to 150 mm; mains that are made of DI and of diameter more than 150 mm; and others. The other group contains pipelines of any sizes that are made of polyvinyl chloride.

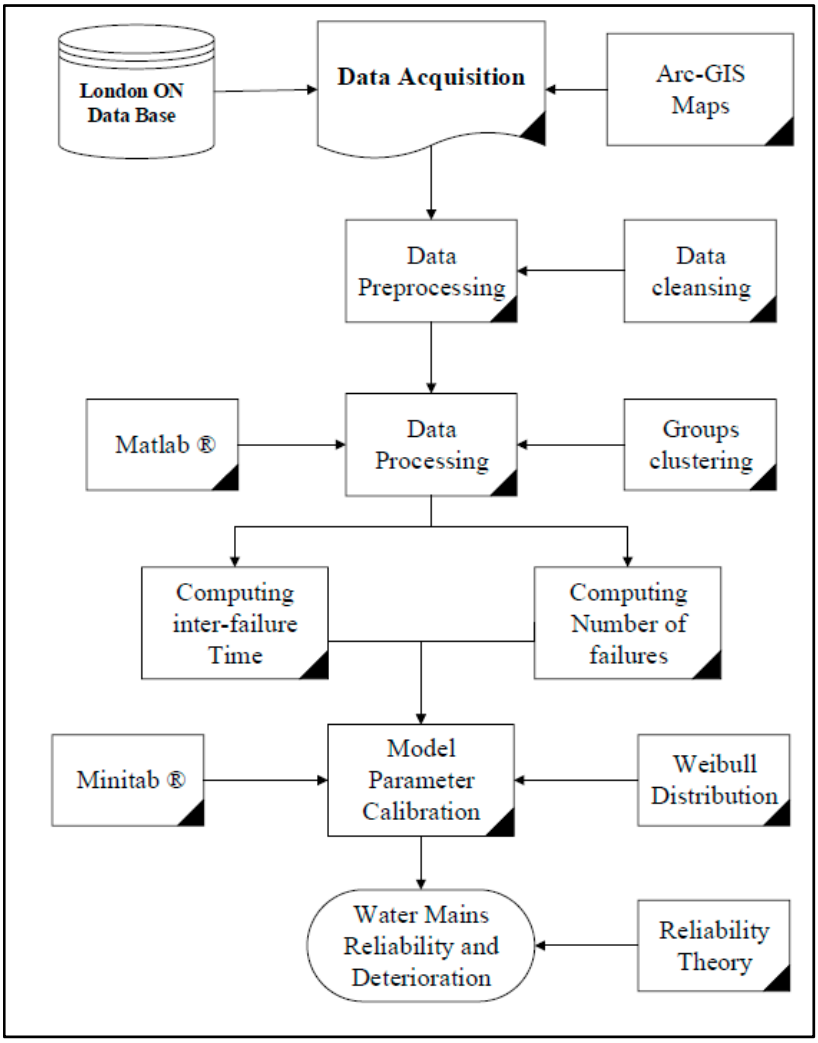

Figure 6. Flow diagram of reliability and deterioration estimation.

Weibull distribution function (WDF) and some other distributions are then employed to estimate the reliability and deterioration of water mains. Weibull distribution is chosen because it is a stochastic statistical failure prediction model based on historical failure data. Unlike Markov-based models in which deterioration is predicted based on the previous condition state only, WDF can utilize the entire failure history of a pipe segment in predicting its deterioration and reliability. This study is

also different than those that assumed a constant failure rate of water pipes. Weibull distribution functions are used in this study to fit the time-to-failure data. The main advantage of this approach is the ability to model the failure of water mains more realistically since failure rates are not constant. Weibull distribution is also chosen as it can be related to several other probability distributions such as exponential, Rayleigh, and other distributions. The probability density function of a three-parameter Weibull distribution is given by Equation (7) [36]:

$$f(T,\beta,\eta,\gamma) = \frac{\beta}{\eta}\left(\frac{T-\gamma}{\eta}\right)^{\beta-1} e^{-\left(\frac{T-\gamma}{\eta}\right)^{\beta}} \quad (7)$$

where: $T \geq 0$, $\beta > 0$, $\eta > 0$, $-\infty \leq \gamma \leq \infty$, T is the time of failure, β is the shape parameter, η is the scale parameter, and γ is the location parameter. Fitting is performed to obtain the Weibull distribution parameters for each transition state using the maximum likelihood method. A state is defined here as the order of break, and the time between states is the time elapsed between the nth break and the $(n + 1)$th break. For instance, the first transition time is the time to the first failure calculated from the installation date. The second transition time is the time to the second failure measured from the date of the first failure, etc. Different distributions were considered to fit the inter-failure time data, such as two-parameter and three-parameter Weibull distributions, exponential distribution, gamma distribution, and others. The quality of each fit is tested using the Anderson–Darling statistical test. Anderson–Darling statistic measures how well the data follow a specific distribution and is used to compare the fit of several distributions to determine the best one. Two main measures are commonly used, namely: the Anderson–Darling statistic (AD) and p-value. A lower AD value and a higher p-value indicate a better fit. Once the Weibull distribution parameters are computed for a cohort of water pipes, the reliability function of this cohort can be calculated as given by Equation (8) [36]:

$$R(T) = e^{-\left(\frac{T-\gamma}{\eta}\right)^{\beta}} \quad (8)$$

where $T \geq 0$ is the duration, $\beta > 0$ is the shape parameter, $\eta > 0$ is the scale parameter, and $-\infty \leq \gamma \leq \infty$ is the location parameter. The last step in this model is to establish the deterioration curves for each cohort of water pipes by incrementally increasing the age in Equation (8). It is worth mentioning that the computed reliability is a time-based one and depends on the break order. As such, if a water pipe experiences its nth break, its reliability along the subsequent years will be calculated using the reliability function of the $(n + 1)$th break.

2.2. Redundancy

Redundancy is the extent to which a system is capable of satisfying functional requirements if significant degradation occurs [50]. Several authors such as Yazdani et al. [51,52] and Torres et al. [28] employed metrics from graph theory to quantify redundancy and connectivity of the WDNs. In graph theory, a network is presented as a mathematical graph $G = (V, E)$ where V is the set of graph nodes with n elements and E is the set of graph edges with m elements. Each edge of G is represented by a pair of nodes (i, j) where $i \neq j$. The size of G is the number n of vertices in V, and the order of G is the number of m edges in E [51,52]. Three different parameters, reported in the literature, are studied to analyze their applicability and limitations in quantifying redundancy of WDNs. These metrics are link density, clustering coefficient, and meshed-ness. Link density is an important measure related to the overall structure of the network. It can be calculated as the ratio between the total and the maximum possible number of links in a network [51,52]. Link density is used to indicate the sparseness or dense-connectivity of network layout, yet it only captures general information regarding the structure of WDNs. Extending the analysis to include other structural properties such as the number of cycles and loops in a network is needed. Clustering coefficient measures the ratio between total triangles and the total connected triples in a network. Because the majority of looped

structures in WDNs are nontriangular, quadrilateral, it is difficult to utilize this metric to measure redundancy in such networks [52]. Meshed-ness is a more relevant metric in this respect that can be used to estimate the intensity of any loops in planar graphs such as WDNs. It may be regarded as a surrogate measure of path redundancy in a network. Meshed-ness is calculated as the ratio of the total number to the maximum number of independent loops in a planar graph Euler's formula, as shown in Equation (9) [52]:

$$R_m = \frac{m - n - 1}{2n - 5} \tag{9}$$

where R_m is meshed-ness coefficient, n is the total number of nodes, and m is the total number of links in a graph G. R_m can vary from zero in tree structures to one in maximal, complete, planar graphs. The value of this coefficient is increased by installing new pipe segments at selected locations across the network. A typical optimization problem can be formulated to select the locations of these newly pipe segments.

2.3. Resilience Metric

The proposed resilience metric is finally formulated as a weighted sum of the robustness and redundancy coefficients that were discussed above, as shown in Equation (10):

$$Я = w_1 \times \frac{\sum_{i=1}^{P} R_i \times C_i}{\sum_{i=1}^{n} C_i} + w_2 \times \frac{m - n - 1}{2n - 5} \tag{10}$$

where $Я$ is the resilience metric, R_i is the reliability of water pipe segment i, C_i is the criticality index of water pipe segment i, P is the total number of pipe segments, n is the network size, m is the network order when presented as graph G, w_1 and w_2 are relative weights of importance. The lower bound of the resilience metric is 0, which is realized when R_i is 0 for all pipe segments in a fully damaged network and no water is being delivered to customers. The theoretical upper bound is 1 and might be realized when R_i is 1 for all pipe segments, and the network is a complete planner graph. In reality, these two cases are not likely to exist, and the expected value of resilience metric is always less than 1.

This metric is not based on a specific hazard and can be used instead to assess the resilience of WDNs based on the failure mode, the impact of the hazard on the network. As mentioned earlier, this effort is focusing only on structural impacts such as pipe breaks. Pipe breaks can result from different hazard events such as earthquakes, target attacks, and accidents. This metric can be used to assess resilience of WDNs in all these types of hazards in a single analysis that investigates the number and individuals of pipes that are broken and the corresponding loss on resilience. Future efforts are considered toward expanding its applicability for other failure modes such as hydraulic failure and water quality-based ones. By including criticality of pipe segments in the proposed formulation, the different social, economic, and environmental consequences of pipe segments failure are assessed. These all are essential dimensions of resilience that still need to be addressed [33]. The reliability estimation model in this formulation is able to stochastically estimate the deterioration of each pipe segment utilizing its previous failure history and other characteristics such as material type, diameter, and failure order. In this model, each time a pipe segment fails or breaks, its reliability and expected duration over the subsequent years are estimated using a new deterioration curve as explained in Section 2.1.2. This approach provides a more accurate estimation of water pipe deterioration which is reflected by the increased failure rate over time and decreased mean time to failure. A precise estimate of pipes' deteriorations is an essential cornerstone in making decisions regarding the maintenance and resilience enhancement of the network during operation and management phase. Such decisions can be obtained by optimizing a resilience metric that explicitly accounts for these factors.

In short, this metric represents a measure of the structural performance of a WDNs in resilience applications. This metric can be used to compare the preparedness level and the ability of different networks to withstand disruptions and continue to function under stressing hazardous events. It can

also be utilized to investigate the gradual increase in resilience during the recovery process. A separate study is being considered to formulate holistic optimization models that utilize this metric in resilience enhancement and recovery applications.

3. Results and Discussions

A real-life water network that serves a selected area in the City of London, Ontario is leveraged in this study for the implementation purposes. The City of London owns a water network over 1500 km in length with a replacement value of more than $2.7 billion [53]. The selected subnetwork serves a specific area in the heart of London downtown. This network is composed of 186 pipe segments that amount approximately 13.1 km of length and has 143 demand nodes. The city of London keeps a rich inventory database of its water network. The oldest active water main that was analyzed in the selected sub-network was installed back in 1905, while the oldest break recorded was in 1974. Figure 7 shows the layout of the selected subnetwork of London Water Distribution Network, referred here as LWDN, which is carefully chosen to provide a vicinity of diverse customers. LWDN is located in a condensed area that serves various residential, commercial, and institutional buildings. LWDN is mainly composed of cast iron (CI) and Polyvinyl chloride (PVC) pipes with diameters ranging from 40 mm to 450 mm. The distributions of the pipe material and size for the LWDN are depicted in Figure 8.

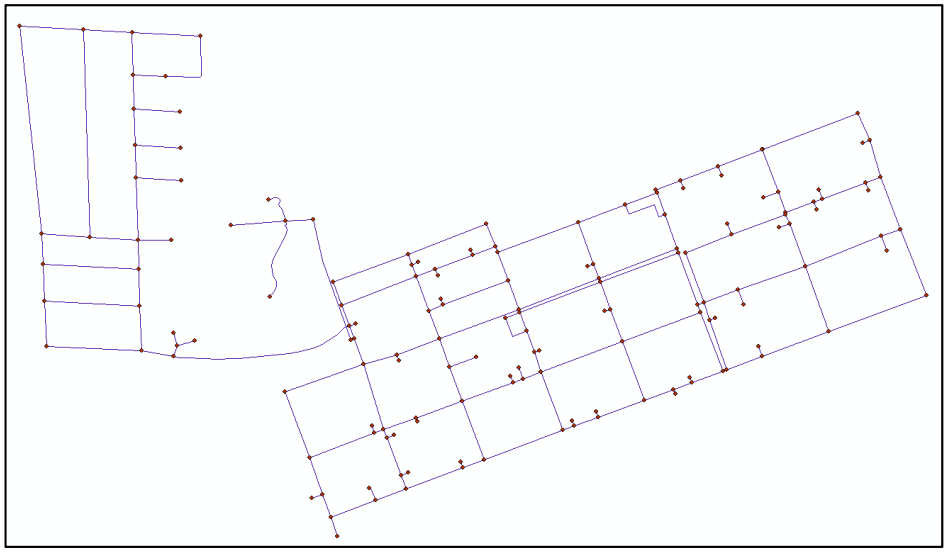

Figure 7. A layout of London Water Distribution Network, LWDN.

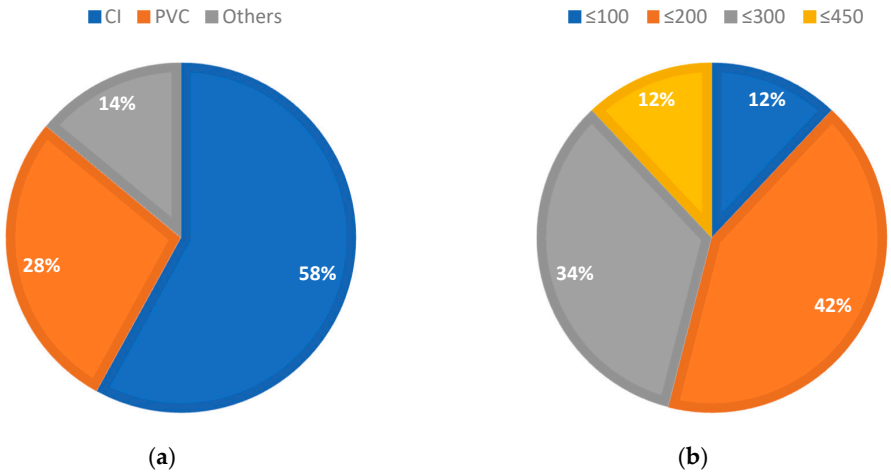

(**a**) (**b**)

Figure 8. LWDN characterization through distribution of pipe: (**a**) material; (**b**) diameter (mm).

This section proceeds in illustrating the results of using the proposed metric in three main resilience applications, namely: assessment, enhancement, and restoration. In the first subsection, the proposed metric is used to assess the resilience of LWDN following the steps mentioned in Section 2. Next, an optimization model is formulated to determine the optimal resilience enhancement plan. The main objective of this optimization framework is to improve the current resilience level of LWDN in order to increase its ability to withstand future disruptions. Subsequently, the proposed metric is utilized in evaluating different restoration strategies after assuming a specific resilience loss in LWDN. The aim of this evaluation is to select the most effective restoration strategy that minimizes the time of service disruption after a hazard occurrence. This three-level implementation demonstrates the practicality and usefulness of integrating the proposed metric in operation and management programs of WDNs both before and after disruption events. In the last subsection, the results are compared to values obtained by previous resilience metrics to highlight main differences and improvements offered by the proposed metric.

3.1. Resilience Assessment

This subsection shows sample calculations to obtain criticality and reliability of a selected pipe segment. Subsequently, the results of all pipe segments in LWDN are integrated to compute the robustness of the network. The redundancy is also added to estimate the resilience level of LWDN.

For criticality calculations, FANP procedure starts with pairwise comparisons between criticality factors before applying the Chang's fuzzifying to construct the upper and lower matrices. Table 3 illustrates the lower, most probable, and upper as calculated for the economic sub-factors. Similar calculations are performed for other sub-factors and the main factors. The lower, upper, and most probable pairwise comparison matrices are then used as inputs to generate the unweighted supermatrix (see Appendix A). A Matlab code was written specifically for this purpose. Weighted supermatrix is then established by normalizing each cell by the summation of the column in which it is located. The last step is to obtain the limited matrix by raising the weighted supermatrix to large powers until convergence. The multiplication was done using Matlab environment where the weighted matrix was multiplied by itself around 1075 times before convergence. A sample of the unweighted, weighted, and limited supermatrix is provided in Appendix A.

Table 3. Economic sub-factors pairwise comparison (lower, most probable, upper).

Factor	Size	Material	Depth	Accessibility
Size	(1,1,1)	(1 1/2,2,2 1/2)	(1,1 1/2,2)	(1/2,1,1 1/2)
Material	(2/5,1/2,2/3)	(1,1,1)	(1/2,1,1 1/2)	(2/5,1/2,2/3)
Depth	(1/2,2/3,1)	(2/3,1,2)	(1,1,1)	(1/2,2/3,1)
Accessibility	(2/3,1,2)	(1 1/2,2,2 1/2)	(1,1 1/2,2)	(1,1,1)

The first column in the limited matrix represents the global weights of importance for each sub-factor. Table 4 shows that the most influential factor in estimating criticality of a pipe segment is its size followed by its accessibility level, the population density, and the type of facility it serves, respectively.

A specific pipe segment is chosen to estimate its criticality for demonstration purposes. This pipe segment is made of ductile iron and has a diameter size of 150 mm. The characteristics and effect values of the selected segment are shown in Table 5. Criticality index of this pipe segment is found to be 0.41 using Equation (5). As mentioned earlier, the effect values for each criticality factor were obtained from experts working in different cities and municipalities across North America.

Table 4. Weights of criticality factors.

Criticality Factor	Weight
Size	0.2703
Accessibility	0.1261
Population density	0.1036
Type of facility	0.0904
Depth	0.0786
Alternative route	0.0767
Soil type	0.0754
Material	0.0685
Traffic disruption	0.0559
Proximity to water streams	0.0544

Table 5. Criticality computation for a pipe segment in LWDN.

Critical Factor	Actual Value	Assigned Value
Size	150 mm	3
Material	Ductile Iron	5
Depth	1.6 m	1
Accessibility	Low	10
Soil type	Sand	10
Proximity to water streams	No	1
Population density	Low	3
Traffic disruption	Low	3
Alternative route	Yes	1
Type of serviced facility	Residential	3

Reliability computations start by calculating the times between breaks for each break order, and curve fitting is applied to obtain the parameters of the best distribution. These parameters are then used to estimate the reliability of pipe segments and generate their deterioration curves. A distinct deterioration curve is associated with each break order. This step is repeated for each cluster of homogenous pipe segments, as stated in Section 2. Pipes are clustered into cohorts to get a more accurate estimation about their reliability and deterioration. Table 6 illustrates a sample of the obtained parameters of Weibull distribution for the group of pipelines that are made of cast iron and of a nominal size that is less than 150 mm, (CI < 150 mm). In this case, a three-parameter Weibull distribution produces a better fitting for data related to time to the first failure, while a two-parameter Weibull distribution yielded sounder fittings for subsequent failures. This is evidenced by the results of the Anderson–Darling (AD) test in which the *p*-values of the three-parameter Weibull distributions are higher, which represent a better fit.

Table 6. Parameters of the Weibull fitting for each state (CI < 150 mm).

State	Shape Parameter η	Scale Parameter β	Location Parameter γ
Time to 1st failure	2.461	62.642	−1.655
Time to 2nd failure	2.221	59.168	−0.214
Time to 3rd failure	2.101	56.249	−0.798
Time to 4th failure	1.756	42.579	−0.430

The value of the shape parameter in each of the previous Weibull distributions is more than one. This value corresponds to an increasing failure rate over time, deteriorating reliability. This phase is known as the wear-out phase or end-life failures, which reflects aged pipe segments. Reliability curve for this cohort (CI < 150 mm) is shown in Figure 9. The age of the selected pipe segment in criticality calculation is 31 years calculated as of this year, 2019. Substituting the shape and scale parameters from Table 6 in Equation (8), the reliability of this specific segment over the following five years is

depicted in Table 7. Reliability is continuously decreasing under the assumption that no maintenance or repair actions are considered for this pipe segment during the planning horizon of the next five years. It is also worth mentioning that this pipe segment will reach a reliability level of 0.751 in five years from today, not the year since it was initially installed.

The overall robustness of the network is then computed by aggregating the reliabilities of all pipe segments and normalizing the summation over the sum of criticalities as given in the first term of Equation (10). Meshed-ness is then calculated to estimate the redundancy of the network. In LWDN, the number of links and nodes are 186 and 143, respectively. Using Equation (9), Meshed-ness R_m for LWDN is then found to be 15.30%. This value indicates a low redundancy level evidenced by the scattered structure of the network as can be observed in Figure 7. This is also due to the existence of a large number of dead-end nodes in the network, almost 25% of the nodes. Dead-end nodes are those connected to dead-end links, that are not part of any loop. This represents an exception to the usual rule because only one link is connected to a node; usually each node is connected to at least 2–3 links. The result of such configuration is an increase in the number of nodes, without a proportional increase in the number of associated links.

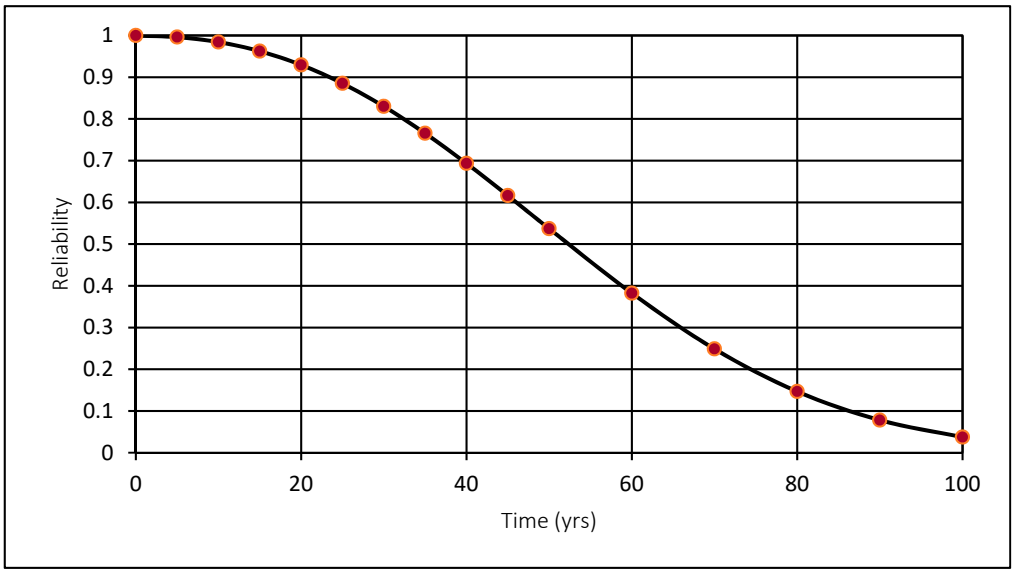

Figure 9. Reliability, survival, behavior for the cohort (CI < 150 mm).

Table 7. Reliability computations for a pipe segment in LWDN.

Year	Age	Reliability (*t*)
0	31	0.818
1	32	0.805
2	33	0.792
3	34	0.779
4	35	0.765
5	36	0.751

The resilience of LWDN is computed by adding redundancy and robustness of the system, each multiplied by a relative weight as per Equation (10). Assuming no resilience enhancement actions are considered over the next five years, the resilience of LWDN is given in Table 8. The resilience of LWDN is found to be 0.467. Besides its structure, which offers little redundancy, this might be related to other factors such as the aging of this network. The average age of pipe segments in LWDN is 75 years, with some segments installed more than 90 years ago. Table 8 shows a continuous decrease in the resilience of LWDN, mainly because of aging and deterioration, when no enhancements actions are considered. As this metric measures the preparedness of LWDN to withstand disruptions and to

continue to supply water to customers, such decrease compromises the network's ability to withstand these disruptions and contributes to extending the periods of services interruptions. This is due to the increased risk of pipe segments failure, especially the most deteriorated ones. For example, a failure of the two most deteriorated segments during a hazard event might cost the city between $142,600 and $166,200 in both direct and indirect costs, because of service interruption and other factors. Estimates were provided by the city's asset management team based on previous incidents and similar deterioration levels. To mitigate these risks, the City of London is expected to take several actions to increase this metric up to a certain acceptable level. Such actions may include a broad spectrum of alternatives for repairing and replacing deteriorated pipe segments in addition to the possibility of installing new segments to increase the network's redundancy. It should be noted that these estimates are based on the local context of the City of London and the set of contractors/suppliers with whom the city is committed. Thus, these estimates might change from one location to another and in the same location, based on different management strategies. The bottom line is that aging and deterioration contribute to decreasing the resilience level and increasing the risk of failure. These risks might be reduced by leading efficient resilience enhancement programs.

Table 8. Resilience of LWDN over the next five years.

Year	Resilience (*t*)
0	0.467
1	0.460
2	0.453
3	0.446
4	0.439
5	0.432

The relative weights of robustness and redundancy that were used in estimating the resilience of LWDN can be changed based on the preference of decision-makers that manage the operation and maintenance of the network. Figure 10 shows the results of sensitivity analysis in which the weights of robustness in Equation (10), and accordingly, weights of redundancy, was changed from 100% to 0%. This analysis is aimed to provide decision-makers with a full understanding of the impacts of the relative weights on resilience metric computations.

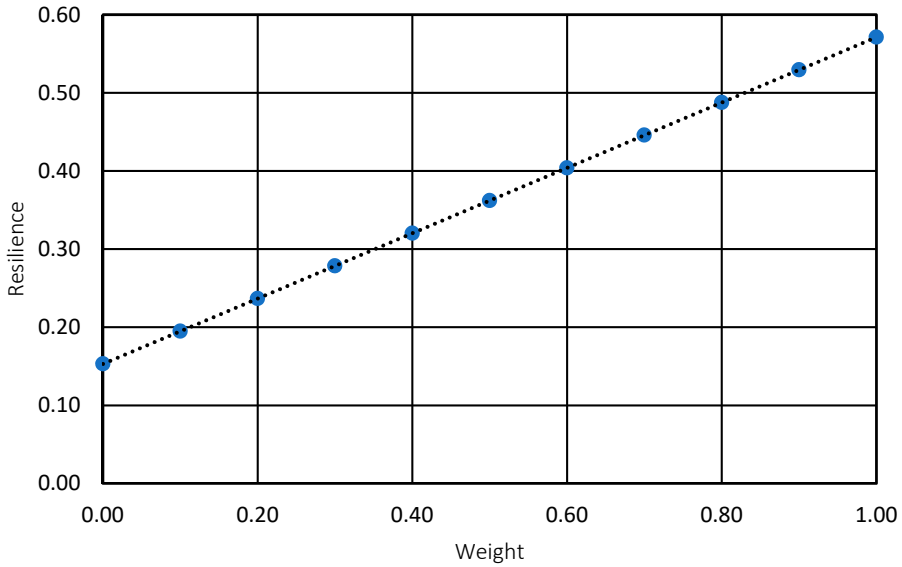

Figure 10. Effect of changing robustness's weight on resilience.

3.2. Resilience Enhancement

An optimization model is formulated in this subsection to determine the optimal strategy for enhancing the resilience of LWDN. The objective of the optimization is to maximize the resilience of LWDN subject to a budget constraint. The resilience of LWDN can be enhanced by increasing its robustness and redundancy. Two main enhancement actions are considered in this framework: replacement of deteriorated pipe segments and installing new ones. Replacement of deteriorated segments improves the network robustness while installing new segments adds redundancy to the network and improves its robustness.

The objective of this optimization framework is to maximize the resilience metric which is given in Equation (10). The budget constraint of the possible enhancement actions is given in Equation (11):

$$C_T = \sum_{i=1}^{N_r} C_i + \sum_{j=1}^{N_j} C_j \leq B_E \tag{11}$$

where C_T = total resilience enhancement cost; N_r = number of pipe segments that need to be replaced; C_i = cost of replacing pipe segment i and it is a function of its length and diameter; N_j = number of newly installed pipe segments; C_j = cost of adding pipe segment j to the network and it is a function of its length and diameter; B_E = available budget for resilience enhancement actions. All pipe segments in LWDN, 186 segments, are considered for replacement. In addition, the nodes of newly installed segments include the set of nodes that are connected to one link only. When a pipe segment is chosen for replacement, the replacing segment is assumed to be of the same diameter as the original one. Also, when a pipe segment is newly installed, its diameter is assumed to be equal to the maximum diameter of the segments connected to any of its end nodes. Lengths of newly installed segments are found by measuring the distance between each two end nodes using the features of Arc-GIS. Reliability of new pipe segments is assumed to be 0.99. This value should theoretically be 1; however, it was reduced to account for installation mistakes and other flaws that could occur in reality and compromise the theoretical value. The unit cost, in Canadian dollar, of replacing a pipe segment is taken as \$1.72/mm/m (per mm of diameter per m of pipe segment length), and the unit cost of new installations is \$3.88/mm/m. These costs were collected from contractors and consultants in Ontario, Canada during 2019, assuming that pipe bursting technique is used for replacement and horizontal directional drilling for new installations.

This study employs genetic algorithm, GA, to determine the optimal, or near-optimal, resilience enhancement plan. GA is a search heuristic inspired by the natural evolution theory that was developed in the late 1960s and early 1970s by John Holland [54]. The model starts by generating a random set of solutions, individuals. Each individual represents a different combination of the decision variables. Solutions are sorted and ranked based on the fitness of each solution compared to other solutions. Best solutions are then selected to undergo the genetic operators of crossover and mutation in order to reproduce and generate a new population of solutions. In cross-over, two parents exchange genes among themselves until the crossover point is reached. The point at which crossover takes places was chosen randomly with a crossover probability of 0.75. In mutation, genes are mutated with low random probability (taken as 0.015) to maintain diversity within the population and prevent premature convergence. These iterative steps are then repeated to ensure convergence to the optimal or near-optimal set of solutions [55].

Figure 11 shows the convergence of the optimization model for a sample budgetary constraint of \$500,000, in which the y-axis represents the resilience of LWDN and the x-axis represents the number of generations after which the model would converge. An optimum value of 0.564 was obtained after 2200 generations, following which no improvement was observed. The optimization algorithm was run on an 8GB RAM, 3.60 GHz i7 core CPU, and Windows 7 with 64-bit operating system. The optimization model run time was 42 s. It was found that replacement actions constitute for about 77%, \$384,500, of the total resilience enhancement budget. This could be referred to the plenty

of existing deteriorated, aged, pipe segments in this subnetwork. As mentioned earlier, several pipe segments in LWDN, around 16%, were installed more than 90 years ago. Replacing such severely deteriorated segments would significantly increase the resilience of LWDN with a relatively cheaper cost than installing new segments; thus such solutions were selected. Resilience enhancement budgets ranging between $200,000 and $1 million, with an increment of $200,000, were then considered to be the budget constraint of the optimization model.

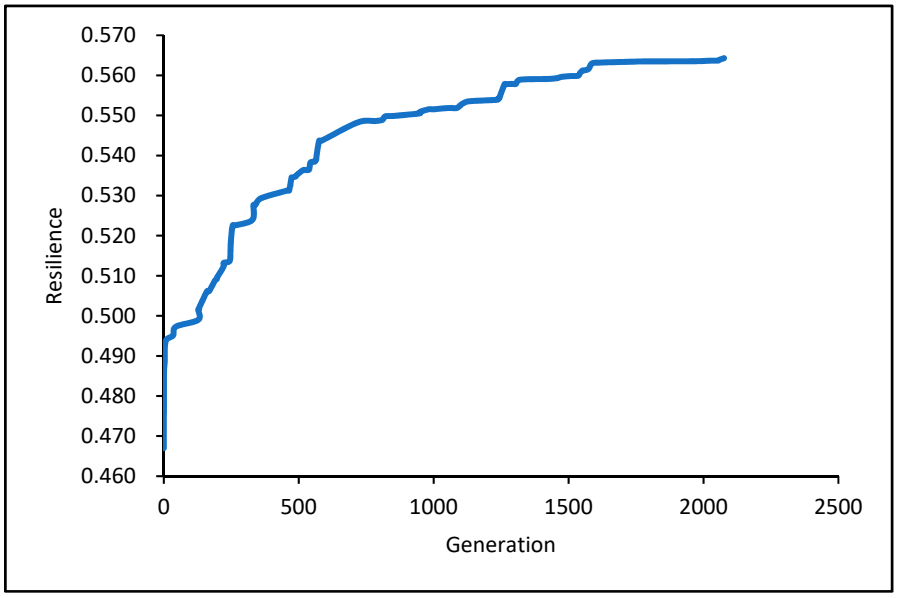

Figure 11. Convergence of the genetic algorithm optimization model.

Figure 12 depicts a trade-off between the resilience of LWDN and costs of resilience enhancement. It can be observed from Figure 12 that resilience of LWDN can be increased to 0.564, by 21%, with a $50,000 investment and to a value of 0.599, by 28%, with a $1 million investment in the resilience enhancement actions. It is worth mentioning that to increase the practicality of installing new pipe segments as a way to enhance resilience, these new installations should be integrated with long-term capital planning.

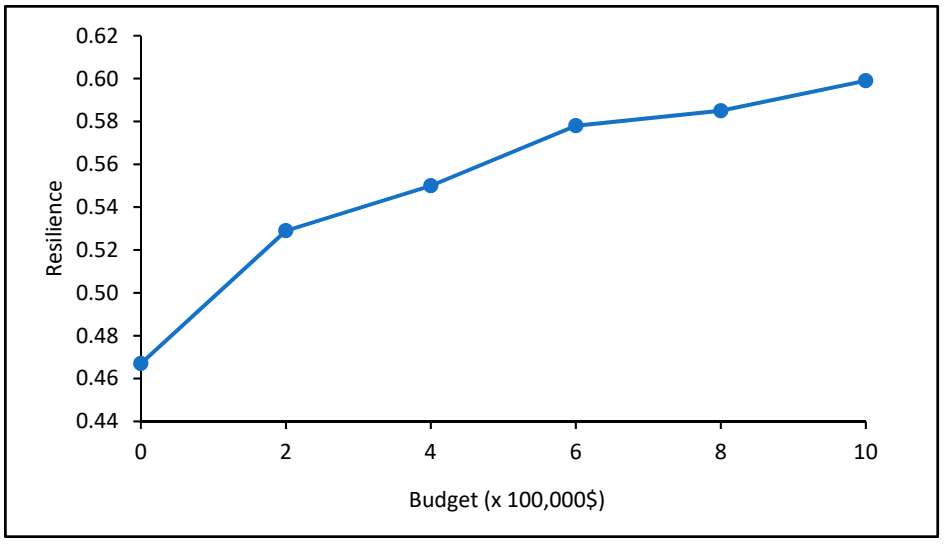

Figure 12. Resilience versus cost trade-off for LWDN.

3.3. Resilience Restoration

To demonstrate the practicality of using the proposed metric during the restoration phase, a simple scenario is discussed below, assuming a disruption event that caused a certain number of segments to fail. In reality, the exact number and individuals of failed pipe segments are random in case of natural disruptions such as earthquakes. Another way of picking individual failed segments is through targeted failure analysis, which is commonly used in security applications. The initial resilience level of 0.467 is used as a reference value, which represents the undisrupted state of LWDN. A disruption event that causes a failure of nine randomly chosen segments is assumed. When a pipe segment fails, its reliability, probability of survival, is reduced to zero in Equation (10), and resilience metric is recalculated. As a result, the resilience of LWDN decreased around 5% to a value of 0.443. It is then required to investigate three possible recovery strategies. Each pipe segment requires a different restoration period based on its size, material type, and external conditions. Pipe bursting technology was considered for replacing the failed pipe segments. Exact restoration durations of each pipe segment were gathered from consultants and contractors in Ontario, Canada. Initial set-up time for the repair team is neglected in this illustration. The relocation time is also ignored in this example; i.e., no time is spent when the repair crew moves from one segment to another. Each restoration strategy specifies the sequence, order, in which pipe segments are being restored. The first strategy is to fix the failed segments based on their criticality in descending order. The second one is to repair the failed segments based on their age from the oldest to the newest pipe segments. The last strategy is to fix the failed segments based on the realized increase in resilience metric, such that those segments that yield the biggest improvement are fixed first. Table 9 describes the state of LWDN after each time step following the first restoration strategy. At t_d, time of disruption, a disruption occurs which causes a sudden resilience drop (in this specific case $t_0 = t_d$). This drop is indicated by a status value of 0 for the failed pipe segments. Pipe segments are then sequentially restored, indicated by a value of 1, from time steps t_1 through t_f, the time step at which restoration actions are accomplished. The increase in resilience over time following restoration strategy 1 is depicted in Table 10. Similar computations can be attained for restoring strategies 2 and 3. Figure 13 illustrates three distinct resilience restoration behaviors for LWDN. For example, the resilience of LWDN reaches a level of 97% of its original value after 16 days following strategy 3 and reaches the same level after 31 and 20 days following strategy 1 and strategy 2, respectively. In general, the third strategy is the fastest in restoring LWDN to its original state. It is worth mentioning that this example is simplified to illustrate the applicability of the proposed resilience metric. However, the distinct behaviors of each strategy imply the importance of developing more reliable methods to determine the best restoration plan. Optimization and other multi-criteria decision-making tools can be utilized to achieve this purpose.

Table 9. LWDN behavior following restoration strategy 1.

Pipe Segment	Status										
	t_0	t_d	t_1	t_2	t_3	t_4	t_5	t_6	t_7	t_8	t_9
34	1	0	1	1	1	1	1	1	1	1	1
148	1	0	0	0	1	1	1	1	1	1	1
76	1	0	0	1	1	1	1	1	1	1	1
161	1	0	0	0	0	1	1	1	1	1	1
56	1	0	0	0	0	0	1	1	1	1	1
42	1	0	0	0	0	0	0	0	1	1	1
130	1	0	0	0	0	0	0	0	0	0	1
185	1	0	0	0	0	0	0	1	1	1	1
1	1	0	0	0	0	0	0	0	0	1	1

Table 10. Resilience computations for strategy 1.

Time (days)	Resilience	Resilience (%)
0	0.467	100.00
0	0.443	94.84
7	0.443	94.89
20	0.445	95.37
23	0.447	95.89
27	0.449	96.13
31	0.452	96.82
32	0.456	97.63
36	0.459	98.46
41	0.463	99.18
53	0.467	100.00

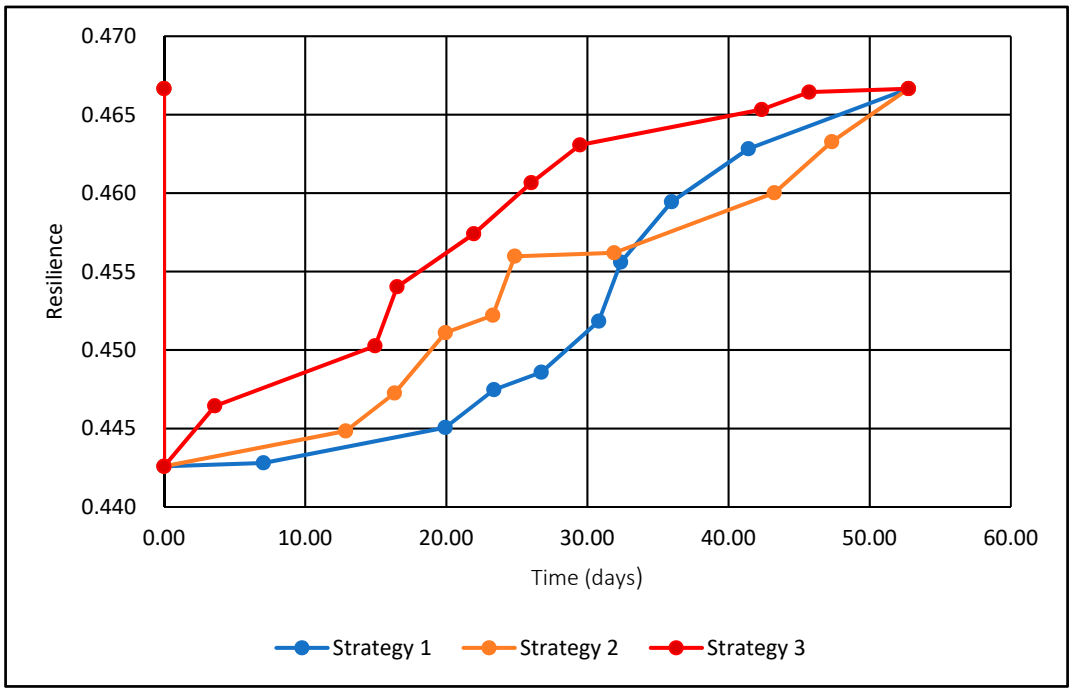

Figure 13. Comparison of three resilience restoring strategies based on the proposed metric.

3.4. Evaluation and Validation

The rest of this section encompasses an evaluation of utilizing the proposed metric in the various resilience applications that were described previously. First, the obtained resilience results of LWDN under different states are compared to those found by a previously developed metric. Second, a hydraulic model is simulated to evaluate the same restoration strategies investigated in the previous subsection. Results are compared to those obtained by the proposed metric, and main differences are discussed.

3.4.1. Metric Validation

As a mean of validation, the estimated resilience level of LWDN is compared to a resilience level obtained by another resilience metric develop by Farahmandfar et al. [1]. Farahmandfar et al. [1] proposed a topology-based metric to assess resilience of WDNs based on robustness and redundancy.

The metric is formulated as the sum of reliabilities of the connected pipelines each multiplied by its nodal demand in a modified form of the original nodal degree as given by Equation (12) [1]:

$$R = \frac{\sum_{i=1}^{N_n} \left\{ \left[\sum_{j=1}^{N_i} (1 - P_{fj}) \right] \times Q_i \right\}}{4 \times \sum_{i=1}^{N_n} Q_i} \quad (12)$$

where N_n = total number of nodes, N_i = total number of links connected to node i, P_{fj} = failure probability of link j, and Q_i = demand of node i. The resilience level of LWDN using this metric was found to be 0.454 compared to a level of 0.467 as found using the proposed metric in this paper. As the concept of resilience is still emerging and being investigated both in academia and in practice, the City of London does not have an estimation of the resilience level of their network yet. Thus, it is not possible to judge which metric is overestimating the resilience level or which metric is outperforming in terms of resilience evaluation. However, the resilience levels of LWDN as obtained by these metrics are quite comparable with the proposed metric yielding a slightly higher, less than 3% increase, resilience level. These results will serve a way of validating the viability of the proposed metric in resilience assessment application of WDNs.

Additionally, resilience levels attained by the two metrics during the different disrupted and enhanced states are compared. This is done to investigate the consistency in the differences between the obtained results and to highlight the main improvements offered by the proposed metric. When the same resilience enhancement actions are applied, the resilience of LWDN, using the metric given by Equation (12), is increased by 19% to a value of 0.540. This is comparable to an increase of 21% obtained using the proposed metric. The difference between the resilience levels of LWDN under the enhanced state as obtained by the two metrics is around 4%. The original resilience level of LWDN, 0.454, is then used as a reference value and the same failure scenario is assumed, a failure of the same nine pipe segments. The resilience of LWDN, using the metric given by Equation (12), as a result decreased 4% to a value of 0.435. This is also comparable to the result obtained by the proposed metric where a reduction of 5% was encountered. The difference between resilience levels of LWDN under the disrupted state is less than 2%. Generally, it is observed that the proposed metric estimates a higher resilience level, which can be referred to the difference between the two metrics in quantifying redundancy. While in their metric, Farahmandfar et al. [1] depend solely on the nodal degree, the proposed metric in this study considers both the number of nodes and links in determining the number of loops in a network, Equation (9). Additionally, Farahmandfar et al. [1] utilized nodal demand as a weighting factor, multiplied by the sum of reliabilities, to highlight the nodes of higher demand. However, the demand can be zero for some nodes based on the network structure. Hence, reliabilities of the segments connected to such nodes will not be counted in resilience estimation. This is avoided in the proposed metric, where criticality of each segment is used as a weighting factor instead of nodal demand. Readers can refer to [56] for more details about zero-demand nodes and the network structure.

3.4.2. Hydraulic Evaluation

A hydraulic model is simulated in this subsection to assess the suitability of using the proposed metric during the restoration phase. The performance of the proposed metric is evaluated using serviceability index *SI*, a frequent used surrogate measure of hydraulic reliability in resilience applications of WDNs [57]. A topological map of LWDN was exported from the Arc-GIS shapefile and fed into WaterGEMS software [58] which was used to build and run the hydraulic simulation model. Nodes' coordinates, pipes' length, diameters, and roughness coefficients were directly extracted from the available layers in the shapefiles. A Google application programming interface (API) was used to access Google Earth from which the user can determine the elevation of any location. Nodes' elevations and estimated nodal demands were then assigned. The model was run, and data regarding the service pressure at each junction were collected. The previously mentioned disrupted scenario was

then analyzed by modeling breaks of the same nine selected pipe segments. In this analysis, a pipe break was modeled by changing its status to closed and evenly distributing a discharge flow to the end nodes as additional demands [31]. Discharge flows were calculated using Equations (13) [31,59]:

$$Q_j = 84.04 \times C_d \times A_j \times P_j^{0.5} \tag{13}$$

where Q_j = discharge from the orifice pipe j; C_d = discharge coefficient (0.8 in this application); A_j = the total cross-sectional area of pipe j; P_j = average pressure of ends nodes of pipe j. There are two main types of hydraulic analysis methods of water systems: demand-driven analysis (DDA) and pressure-driven analysis (PDA) [57]. DDA is more suitable for analysis under normal conditions as they assume that demands at junctions are always satisfied which might result in unrealistic negative pressure values [57]. PDA, on the other hand, is preferred in analyzing abnormal conditions as they assume that the demand is a function of the pressure, and thus, unrealistic values can be avoided. However, PDA application requires assuming a head-outflow relationship (HOR) for each network as there is no such universally accepted relationship [57,60]. In this simulation, quasi-PDA is employed to deal with negative pressure that might occur during the disrupted state of the network based on the same methodology used by Yoo et al. [57]. In this approach, whenever a negative pressure is encountered at a node, the demand at that node is set to zero, and the simulation is repeated. If negative pressure reoccurred, the calculated pressure is assumed zero. Serviceability index of the system *SI* is used to estimate the reliability of the network based on Equations (14) and (15) [57]:

$$SI = \frac{\sum_{i=1}^{n} Q_{avl,i}}{\sum_{i=1}^{n} Q_{req,i}} \tag{14}$$

$$Q_{avl,i} = \begin{cases} 0, & \text{when } P_i \le 0 \\ Q_{new,i} \times \sqrt{\dfrac{P_i}{P_{min}}}, & \text{when } 0 \le P_i \le P_{min} \\ Q_{new,i}, & \text{when } P_i \ge P_{min} \end{cases} \tag{15}$$

where $Q_{avl,i}$ = available demand at node i; $Q_{req,i}$ = required demand at node i; $Q_{new,i}$ = updated nodal demand after considering the disrupted state and dealing with the negative pressure at node i; P_i = nodal pressure at node i; P_{min} = allowable minimum nodal pressure (assumed 15 m in this study); n = number of nodes. Finally, the network was restored three times based on the same restoration strategies mentioned earlier. In each time, the pipe segments were gradually reopened, the assigned flow discharge was removed, and *SI* index was iteratively computed. Figure 14 shows three different restoration behaviors of *SI* from a value of 0.835 to the original value. Restoration strategy 3 yields the fastest rate at which *SI* was recovered as shown in Figure 14. This strategy suggests restoring the failed segments based on the improvement in the proposed resilience metric. Figures 13 and 14 also show different relative behavior for strategy 1 and strategy 2 toward the last three restoration actions, which might need further investigation. However, as the primary objective after a service interruption is to restore the system rapidly, the proposed metric has shown similar results to those obtained by *SI* on this regard, fastest recovery. This shows the potentiality of using the proposed metric as a proxy indicator for *SI*. The use of the proposed metric requires much less computational time in investigating and selecting the best restoration strategy during the recovery phase. In a real application, this can be assured through an optimization model that determines the fastest restoration plan. Such optimization models can be formulated to search over all possible restoration strategies in terms of the order and method of restoring each failed segment. This way, network managers can be more confident about their decisions, since all possible strategies have been considered.

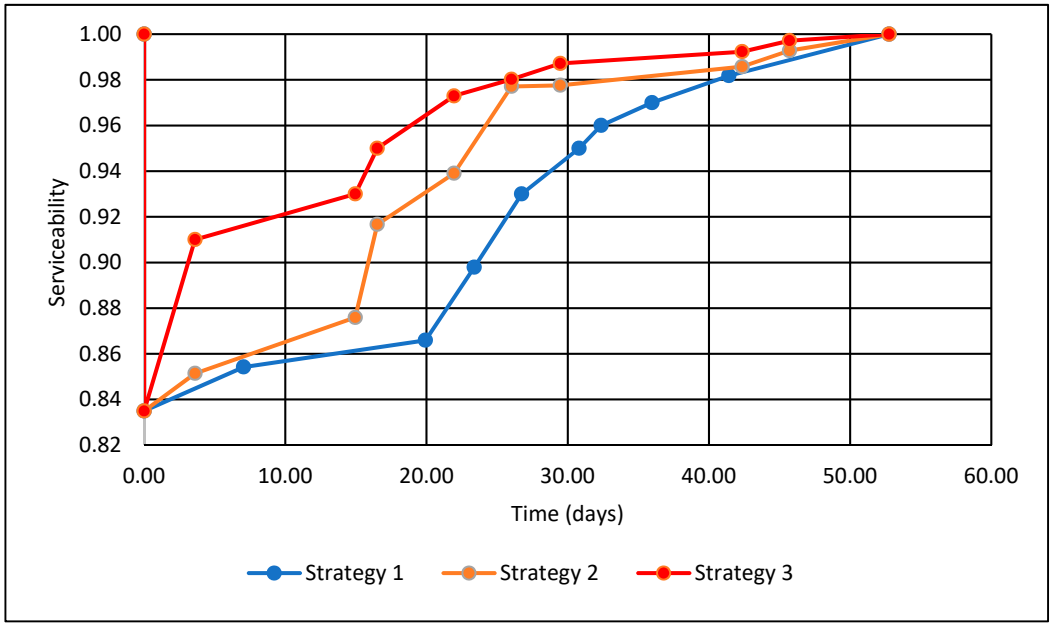

Figure 14. Comparison of three resilience restoring strategies based on serviceability.

4. Conclusions

Water distribution networks (WDNs) are in a deteriorated state, which increases their vulnerability to natural and anthropogenic hazards. These hazards are becoming more frequent and of more destructive consequences. This paper presents a new metric that can be readily used by utilities and asset managers to assess resilience of WDNs before, during, and after hazards. The developed metric captures two main features of resilience: robustness and redundancy. Structural reliability of pipe segments is used to assess the robustness of WDNs. Criticality of each segment is incorporated in the formulation to emphasize segments of higher economic, social, and environmental criticality. Attributes from graph theory are studied and utilized to quantify redundancy in WDNs. Section of a real WDN that serves the City of London, Ontario is leveraged to demonstrate and validate the applicability of this metric. The resilience level of the assessed network is found to be 0.467 compared to a level of 0.454 as estimated by a previously developed metric. A budget-constrained optimization model is formulated to determine the optimal resilience enhancement strategy. A set of resilience enhancement actions valued around $500,000 is found to increase the resilience of LWDN by around 20%. A disruptive scenario that caused a failure of nine randomly selected pipe segments is then assumed. Subsequently, three different restoring strategies are analyzed and compared. The effect of each restoration strategy on the *SI*, a hydraulic reliability measure, is also investigated. City managers can use the proposed metric in assessing and enhancing resilience of the WDNs to improve their ability to withstand disruptions. Results obtained in this study also proves the practicality and usefulness of using the proposed metric in selecting efficient restoration strategies without the need to run complex simulation models.

A limitation of this research is the analysis of structural impacts exclusively. Future efforts are meant to extend its applicability to include the hydraulic effects and water-quality related issues. For example, adding the service pressure to the formulation can help in accurate estimation of hydraulic performance loss, which is beyond the objective of this paper. Also, more factors can be employed in estimating the criticality of water pipe segments, such as pipe thickness. This study focused on water pipelines as they constitute the biggest majority of components; however, it can be extended to include other elements of water networks. For example, the robustness of each pipe segment can be modified to consider the reliability and criticality of other components existing within a segment such as pumps, valves, hydrants, etc. Previous failure history of such components may be utilized in estimating their

reliability. Different methods can be investigated to aggregate the individual components' reliabilities and obtain an indication of the overall segment robustness. Additionally, the redundancy should account for the available number and functionality of other elements in the network. As an extension to this work, the authors are currently utilizing this metric along with different dimensions of resilience such as rapidity and resourcefulness to develop an optimization model for prioritizing and scheduling of restoration actions. Moreover, other resilience improvement measures are being investigated in long-term resilience enhancement planning.

Author Contributions: All the authors contributed to the development of this study. A.A. is a Ph.D. candidate; he developed the proposed metric along with its main analytical quantifications under the close supervision of the other authors. Both O.M. and T.Z. provided valuable insights, additions, and modifications in the development and implementation process. They have also reviewed and edited the original manuscript that was written by A.A. All authors read and approved the final manuscript.

Funding: This research received no external funding.

Acknowledgments: The authors would like to thank Khalid Shahata, Corporate Asset Manager, at the City of London, Ontario, for providing the data needed for the development and implementation purposes. His valuable insights about the current practices of managing and maintaining the WDN at the City of London are highly appreciated. The authors would also like to thank the anonymous reviewers for their helpful and constructive comments that helped in improving the final version of the paper.

Conflicts of Interest: The authors declare no conflict of interest.

Appendix A

This section provides a sample of unweighted, weighted, and limited matrices. These matrices were obtained in the steps of finding the weights of criticality factors following the fuzzy analytical network process technique. These weights are used in Equation (5) to find the criticality index of each pipe segment.

Table A1. Unweighted supermatrix.

	WMC [1]	EF [2]	EVF [3]	SF [4]	S [5]	M [6]	ID [7]	A [8]	S	ST [9]	WS [10]	D [11]	TD [12]	AR [13]	TF [14]
WMC	0	0	0	0	0	0	0	0	0	0	0	0	0	0	0
EF	0.425	0	0.667	0.60	0	0	0	0	0	0	0	0	0	0	0
EVF	0.253	0.40	0	0.40	0	0	0	0	0	0	0	0	0	0	0
SF	0.322	0.60	0.333	0	0	0	0	0	0	0	0	0	0	0	0
S	0	0.319	0	0	1.0	0	0	0	0	0	0	0	0	0	0
M	0	0.171	0	0	0	1.0	0	0	0	0	0	0	0	0	0
ID	0	0.196	0	0	0	0	1.0	0	0	0	0	0	0	0	0
A	0	0.314	0	0	0	0	0	1.0	0	0	0	0	0	0	0
S	0	0	0.523	0	0	0	0	0	1.0	0	0	0	0	0	0
ST	0	0	0.277	0	0	0	0	0	0	1.0	0	0	0	0	0
WS	0	0	0.200	0	0	0	0	0	0	0	1.0	0	0	0	0
D	0	0	0	0.317	0	0	0	0	0	0	0	1.0	0	0	0
TD	0	0	0	0.171	0	0	0	0	0	0	0	0	1.0	0	0
AR	0	0	0	0.235	0	0	0	0	0	0	0	0	0	1.0	0
TF	0	0	0	0.277	0	0	0	0	0	0	0	0	0	0	1.0

[1] Water mains criticality; [2] economic factors; [3] environmental factors; [4] social factors; [5] pipeline size; [6] pipeline material; [7] installation depth; [8] accessibility; [9] soil type; [10] proximity to water streams; [11] population density; [12] traffic disruption; [13] alternative route; [14] type of facility.

Table A2. Weighted supermatrix.

	WMC [1]	EF [2]	EVF [3]	SF [4]	S [5]	M [6]	ID [7]	A [8]	S	ST [9]	WS [10]	D [11]	TD [12]	AR [13]	TF [14]
WMC	0	0	0	0	0	0	0	0	0	0	0	0	0	0	0
EF	0.425	0	0.333	0.300	0	0	0	0	0	0	0	0	0	0	0
EVF	0.253	0.200	0	0.200	0	0	0	0	0	0	0	0	0	0	0
SF	0.322	0.300	0.167	0	0	0	0	0	0	0	0	0	0	0	0
S	0	0.160	0	0	1.0	0	0	0	0	0	0	0	0	0	0
M	0	0.085	0	0	0	1.0	0	0	0	0	0	0	0	0	0
ID	0	0.098	0	0	0	0	1.0	0	0	0	0	0	0	0	0
A	0	0.157	0	0	0	0	0	1.0	0	0	0	0	0	0	0
S	0	0	0.261	0	0	0	0	0	1.0	0	0	0	0	0	0
ST	0	0	0.139	0	0	0	0	0	0	1.0	0	0	0	0	0
WS	0	0	0.100	0	0	0	0	0	0	0	1.0	0	0	0	0
D	0	0	0	0.159	0	0	0	0	0	0	0	1.0	0	0	0
TD	0	0	0	0.086	0	0	0	0	0	0	0	0	1.0	0	0
AR	0	0	0	0.117	0	0	0	0	0	0	0	0	0	1.0	0
TF	0	0	0	0.138	0	0	0	0	0	0	0	0	0	0	1.0

[1] Water mains criticality; [2] economic factors; [3] environmental factors; [4] social factors; [5] pipeline size; [6] pipeline material; [7] installation depth; [8] accessibility; [9] soil type; [10] proximity to water streams; [11] population density; [12] traffic disruption; [13] alternative route; [14] type of facility.

Table A3. Limited matrix.

	WMC [1]	**EF** [2]	**EVF** [3]	**SF** [4]	**S** [5]	**M** [6]	**ID** [7]	**A** [8]	**S**	**ST** [9]	**WS** [10]	**D** [11]	**TD** [12]	**AR** [13]	**TF** [14]
WMC	0	0	0	0	0	0	0	0	0	0	0	0	0	0	0
EF	0	0	0	0	0	0	0	0	0	0	0	0	0	0	0
EVF	0	0	0	0	0	0	0	0	0	0	0	0	0	0	0
SF	0	0	0	0	0	0	0	0	0	0	0	0	0	0	0
S	0.128	0.198	0.078	0.075	1.0	0	0	0	0	0	0	0	0	0	0
M	0.068	0.106	0.042	0.040	0	1.0	0	0	0	0	0	0	0	0	0
ID	0.079	0.121	0.048	0.046	0	0	1.0	0	0	0	0	0	0	0	0
A	0.126	0.195	0.077	0.074	0	0	0	1.0	0	0	0	0	0	0	0
S	0.142	0.087	0.305	0.087	0	0	0	0	1.0	0	0	0	0	0	0
ST	0.075	0.046	0.162	0.046	0	0	0	0	0	1.0	0	0	0	0	0
WS	0.054	0.033	0.117	0.033	0	0	0	0	0	0	1.0	0	0	0	0
D	0.104	0.068	0.054	0.190	0	0	0	0	0	0	0	1.0	0	0	0
TD	0.056	0.037	0.029	0.102	0	0	0	0	0	0	0	0	1.0	0	0
AR	0.077	0.050	0.040	0.140	0	0	0	0	0	0	0	0	0	1.0	0
TF	0.090	0.059	0.047	0.166	0	0	0	0	0	0	0	0	0	0	1.0

[1] Water mains criticality; [2] economic factors; [3] environmental factors; [4] social factors; [5] pipeline size; [6] pipeline material; [7] installation depth; [8] accessibility; [9] soil type; [10] proximity to water streams; [11] population density; [12] traffic disruption; [13] alternative route; [14] type of facility.

References

1. Farahmandfar, Z.; Piratla, K.R.; Andrus, R.D. Resilience evaluation of water supply networks against seismic hazards. *J. Pipeline Syst. Eng. Pract.* **2016**, *8*, 04016014. [CrossRef]
2. Klise, K.A.; Murray, R.; Walker, L.T.N. *Systems Measures of Water Distribution System Resilience*; Sandia National Lab: Albuquerque, NM, USA, 2015.
3. Diao, K.; Sweetapple, C.; Farmani, R.; Fu, G.; Ward, S.; Butler, D. Global resilience analysis of water distribution systems. *Water Res.* **2016**, *106*, 383–393. [CrossRef] [PubMed]
4. Cimellaro, G.P.; Tinebra, A.; Renschler, C.; Fragiadakis, M. New resilience index for urban water distribution networks. *J. Struct. Eng.* **2015**, *142*, C4015014. [CrossRef]
5. Vugrin, E.D.; Warren, D.E.; Ehlen, M.A. A resilience assessment framework for infrastructure and economic systems: Quantitative and qualitative resilience analysis of petrochemical supply chains to a hurricane. *Process Saf. Prog.* **2011**, *30*, 280–290. [CrossRef]
6. Ayyub, B.M. Systems resilience for multihazard environments: Definition, metrics, and valuation for decision making. *Risk Anal.* **2014**, *34*, 340–355. [CrossRef] [PubMed]
7. Hosseini, S.; Barker, K.; Ramirez-Marquez, J.E. A review of definitions and measures of system resilience. *Reliab. Eng. Syst. Saf.* **2016**, *145*, 47–61. [CrossRef]
8. Fisher, R.E.; Bassett, G.W.; Buehring, W.A.; Collins, M.J.; Dickinson, D.C.; Eaton, L.K.; Haffenden, R.A.; Hussar, N.E.; Klett, M.S.; Lawlor, M.A. *Constructing a Resilience Index for the Enhanced Critical Infrastructure Protection Program*; Decision and Information Sciences; Argonne National Lab (ANL): Lemont, IL, USA, 2010.
9. Fiksel, J.; Goodman, I.; Hecht, A. Resilience: Navigating toward a sustainable future. *Solutions* **2014**, *5*, 38–47.
10. Todini, E. Looped water distribution networks design using a resilience index based heuristic approach. *Urban Water* **2000**, *2*, 115–122. [CrossRef]
11. Jayaram, N.; Srinivasan, K. Performance-based optimal design and rehabilitation of water distribution networks using life cycle costing. *Water Resour. Res.* **2008**, *44*. [CrossRef]
12. Suribabu, C.R. Resilience-based optimal design of water distribution network. *Appl. Water Sci.* **2017**, *7*, 4055–4066. [CrossRef]
13. Choi, Y.H.; Kim, J.H. Development of Multi-Objective Optimal Redundant Design Approach for Multiple Pipe Failure in Water Distribution System. *Water* **2019**, *11*, 553. [CrossRef]
14. Creaco, E.; Franchini, M.; Todini, E. Generalized resilience and failure indices for use with pressure-driven modeling and leakage. J. *Water Resour. Plan. Manag.* **2016**, *142*, 04016019. [CrossRef]
15. Bruneau, M.; Chang, S.E.; Eguchi, R.T.; Lee, G.C.; O'Rourke, T.D.; Reinhorn, A.M.; Shinozuka, M.; Tierney, K.; Wallace, W.A.; Von Winterfeldt, D. A framework to quantitatively assess and enhance the seismic resilience of communities. *Earthq. Spectra* **2003**, *19*, 733–752. [CrossRef]
16. Sahebjamnia, N.; Torabi, S.A.; Mansouri, S.A. Integrated business continuity and disaster recovery planning: Towards organizational resilience. *Eur. J. Oper. Res.* **2015**, *242*, 261–273. [CrossRef]
17. Adams, T.M.; Bekkem, K.R.; Toledo-Durán, E.J. Freight resilience measures. *J. Transp. Eng.* **2012**, *138*, 1403–1409. [CrossRef]
18. Henry, D.; Ramirez-Marquez, J.E. Generic metrics and quantitative approaches for system resilience as a function of time. *Reliab. Eng. Syst. Saf.* **2012**, *99*, 114–122. [CrossRef]
19. Cutter, S.L.; Barnes, L.; Berry, M.; Burton, C.; Evans, E.; Tate, E.; Webb, J. A place-based model for understanding community resilience to natural disasters. *Glob. Environ. Chang.* **2008**, *18*, 598–606. [CrossRef]
20. Pant, R.; Barker, K.; Ramirez-Marquez, J.E.; Rocco, C.M. Stochastic measures of resilience and their application to container terminals. *Comput. Ind. Eng.* **2014**, *70*, 183–194. [CrossRef]
21. Dessavre, D.G.; Ramirez-Marquez, J.E.; Barker, K. Multidimensional approach to complex system resilience analysis. *Reliab. Eng. Syst. Saf.* **2016**, *149*, 34–43. [CrossRef]
22. Ouyang, M.; Dueñas-Osorio, L.; Min, X. A three-stage resilience analysis framework for urban infrastructure systems. *Struct. Saf.* **2012**, *36*, 23–31. [CrossRef]
23. Zhao, X.; Chen, Z.; Gong, H. Effects comparison of different resilience enhancing strategies for municipal water distribution network: A multidimensional approach. *Math. Probl. Eng.* **2015**, *2015*, 438063. [CrossRef]
24. Baroud, H.; Barker, K.; Ramirez-Marquez, J.E. Importance measures for inland waterway network resilience. *Transp. Res. Part E Logist. Transp. Rev.* **2014**, *62*, 55–67. [CrossRef]

25. Laucelli, D.; Giustolisi, O. Vulnerability assessment of water distribution networks under seismic actions. *J. Water Resour. Plan. Manag.* **2014**, *141*, 04014082. [CrossRef]
26. Cimorelli, L.; Morlando, F.; Cozzolino, L.; D'Aniello, A.; Pianese, D. Comparison among resilience and entropy index in the optimal rehabilitation of water distribution networks under limited-budgets. *Water Resour. Manag.* **2018**, *32*, 3997–4011. [CrossRef]
27. Yazdani, A.; Otoo, R.A.; Jeffrey, P. Resilience enhancing expansion strategies for water distribution systems: A network theory approach. *Environ. Model. Softw.* **2011**, *26*, 1574–1582. [CrossRef]
28. Torres, J.M.; Duenas-Osorio, L.; Li, Q.; Yazdani, A. Exploring topological effects on water distribution system performance using graph theory and statistical models. *J. Water Resour. Plan. Manag.* **2016**, *143*, 04016068. [CrossRef]
29. Diestel, R. *Graph Theory*; Springer: Berlin/Heidelberg, Germany, 2005.
30. Bruneau, M. Enhancing the resilience of communities against extreme events from an earthquake engineering perspective. *J. Secur. Educ.* **2006**, *1*, 159–167. [CrossRef]
31. Farahmandfar, Z.; Piratla, K.R. Comparative Evaluation of Topological and Flow-Based Seismic Resilience Metrics for Rehabilitation of Water Pipeline Systems. *J. Pipeline Syst. Eng. Pract.* **2017**, *9*, 04017027. [CrossRef]
32. Shuang, Q.; Liu, H.J.; Porse, E. Review of the Quantitative Resilience Methods in Water Distribution Networks. *Water* **2019**, *11*, 1189. [CrossRef]
33. Shin, S.; Lee, S.; Judi, D.; Parvania, M.; Goharian, E.; McPherson, T.; Burian, S. A systematic review of quantitative resilience measures for water infrastructure systems. *Water* **2018**, *10*, 164. [CrossRef]
34. O'Rourke, T.D. Critical infrastructure, interdependencies, and resilience. *BRIDGE-Wash.-Natl. Acad. Eng.* **2007**, *37*, 22.
35. Bocchini, P.; Frangopol, D.M. Thomas Ummenhofer, and Tim Zinke. Resilience and sustainability of civil infrastructure: Toward a unified approach. *J. Infrastruct. Syst.* **2013**, *20*, 04014004. [CrossRef]
36. Murthy, D.P.; Rausand, M.; Østerås, T. *Product Reliability: Specification and Performance*; Springer Science Business Media: Berlin/Heidelberg, Germany, 2008.
37. Verma, A.K.; Ajit, S.; Karanki, D.R. *Reliability and Safety Engineering*; Springer Series in Reliability Engineering; Springer: London, UK, 2010.
38. Cromwell, J.E. *Costs of Infrastructure Failure*; American Water Works Association: Denver, CO, USA, 2002.
39. Vanier, D.J.; Rahman, S. *A Primer on Municipal Infrastructure Asset Management*; NSERC: Ottawa, ON, Canada, 2004.
40. Salman, A. Reliability-Based Management of Water Distribution Networks. Ph.D. Thesis, Building, Civil, and Environmental Engineering Department, Concordia University, Montreal, QC, Canada, 2011.
41. Atef, A. Optimal Condition Assessment Policies for Water and Sewer Infrastructure. Master's Thesis, Nile University, Cairo, Egypt, 2010.
42. Moursi, A. Priority Assessment Model for Water Distribution Networks. Master's Thesis, Building, Civil, and Environmental Engineering Department, Concordia University, Montreal, QC, Canada, 2016.
43. Işıklar, G.; Büyüközkan, G. Using a multi-criteria decision making approach to evaluate mobile phone alternatives. *Comput. Stand. Interfaces* **2007**, *29*, 265–274. [CrossRef]
44. Wei, J.; Sun, A.; Wang, C. The application of fuzzy-ANP in the selection of supplier in supply chain management. In Proceedings of the 2010 International Conference on Logistics Systems and Intelligent Management (ICLSIM), Harbin, China, 9–10 January 2010; Volume 3, pp. 1357–1360.
45. Cheng, C.H.; Yang, K.L.; Hwang, C.L. Evaluating attack helicopters by AHP based on linguistic variable weight. *Eur. J. Oper. Res.* **1999**, *116*, 423–435. [CrossRef]
46. Kahraman, C.; Ertay, T.; Büyüközkan, G. A fuzzy optimization model for QFD planning process using analytic network approach. *Eur. J. Oper. Res.* **2006**, *171*, 390–411. [CrossRef]
47. Kiriş, Ş. Multi-criteria inventory classification by using a fuzzy analytic network process (ANP) approach. *Informatica* **2013**, *24*, 199–217.
48. Mohammed, A.U. Integrated Reliability Assessment of Water Distribution Networks. Master's Thesis, Building, Civil, and Environmental Engineering Department, Concordia University, Montreal, QC, Canada, 2016.
49. Gheisi, A.; Forsyth, M.; Naser, G. Water distribution systems reliability: A review of research literature. *J. Water Resour. Plan. Manag.* **2016**, *142*, 04016047. [CrossRef]

50. Tierney, K.; Bruneau, M. Conceptualizing and measuring resilience: A key to disaster loss reduction. *TR News* **2007**, *250*, 14–17.
51. Yazdani, A.; Jeffrey, P. Water distribution system vulnerability analysis using weighted and directed network models. *Water Resour. Res.* **2012**, *48*. [CrossRef]
52. Yazdani, A.; Jeffrey, P. Complex network analysis of water distribution systems. *Chaos Interdiscip. J. Nonlinear Sci.* **2011**, *21*, 016111. [CrossRef]
53. City of London, Ontario. State of Infrastructure Report. 2013. Available online: https://www.london.ca/city-hall/master-plans-reports/reports/Pages/State-of-Infrastructure-Report.aspx (accessed on 1 March 2019).
54. Holland John, H. *Adaptation in Natural and Artificial Systems*; University of Michigan Press: Ann Arbor, MI, USA, 1975.
55. Goldberg, D.E. *Genetic and Evolutionary Algorithms in the Real World*; IlliGAL Report 99013; University of Illinois at Urbana-Champaign, Illinois Genetic Algorithms Laboratory: Urbana, IL, USA, 1999.
56. Bahadur, R.; Johnson, J.; Janke, R.; Samuels, W.B. Impact of model skeletonization on water distribution model parameters as related to water quality and contaminant consequence assessment. In Proceedings of the Eighth Annual Water Distribution Systems Analysis Symposium (WDSA), Cincinnati, OH, USA, 27–30 August 2016; pp. 1–10.
57. Yoo, D.G.; Jung, D.; Kang, D.; Kim, J.H.; Lansey, K. Seismic hazard assessment model for urban water supply networks. *J. Water Resour. Plan. Manag.* **2015**, *142*, 04015055. [CrossRef]
58. Bentley Systems Incorporated. *WaterGEMS v8Users Manual*; Haestad Methods Solution Center, 27; Siemon Company Dr.: Watertown, CT, USA, 2006.
59. Tabesh, M.; Yekta, A.A.; Burrows, R. An integrated model to evaluate losses in water distribution systems. *Water Res. Manag.* **2009**, *23*, 477–492. [CrossRef]
60. Mays, L.W. *Water Supply Systems Security*; McGraw-Hill: New York, NY, USA, 2003.